Editors' Suggestion

On granular flows: From kinetic theory to inertial rheology and nonlocal constitutive models

Diego Berzi*

Department of Civil and Environmental Engineering, Politecnico di Milano, Milano 20133, Italy

(Received 11 December 2023; accepted 23 February 2024; published 20 March 2024)

Previous results of discrete simulations of steady, unidirectional particle flows, here collected and critically reanalyzed, permit to make the case that the kinetic theory of granular gases, extended to include the correlations in the velocity fluctuations and the role of friction in collisions, provides the long-sought universal framework to predict the flow of realistic particles over the entire range of solid volume fraction from dilute to very dense—the upper limit being the critical value at which rate-independent components of the stresses arise. The case is made even stronger by the explicit derivation of the popular inertial rheology and its nonlocal extension to deal with heterogeneities based on the granular fluidity concept as special limits of the kinetic theory. In the process, common statements about the frictional-collisional duality in the granular stresses and the importance of long-lasting contacts creating a percolating network are shown to be greatly exaggerated for granular flows in practical applications.

DOI: 10.1103/PhysRevFluids.9.034304

I. INTRODUCTION

Granular materials are assemblies of solid particles that dissipate energy whenever they interact and for which Brownian motion is irrelevant [1]. Because of the dissipative nature of their interactions, an external input energy is required to support their motion. Granular materials are ubiquitous in countless industrial and geophysical applications (from the manufacturing of tablets and pills in the pharmaceutical industries to the propagation of landslides and snow avalanches on Earth and other planetary bodies), and have been presented as a proxy to understand the behavior of other disordered athermal systems such as foams, emulsions, and glasses [2].

The scientific interest in granular materials sparked from the pioneering works of Bagnold [3–5] in the mid-20th century, especially in the engineering community interested in the modeling of sediment transport. The grains are almost always immersed in a fluid, but for a handful of applications in astrophysics [6]. Nonetheless, there are situations in which the role of the interstitial fluid can be neglected [7], and this permits to focus on the solid particles only, without confounding effects such as drag, lift, and buoyancy [8].

Depending on how much space is filled with grains, locally measured by the solid volume fraction, the solid particles can be observed with the naked eye (i) to bounce off each other in a seemingly random fashion, that is reminiscent of the classical picture of molecular gases [9], or (ii) to form static or quasistatic assemblies of disordered grains characterized by a network of long-lasting contacts that spans the entire domain [10], perhaps slowly deforming under shear [11]. Accordingly, the granular material is either a granular gas, subjected to rapid deformations, or a granular packing, subjected to slow deformations. Granular packings and their quasistatic motion

*diego.berzi@polimi.it

have been one of the main subjects of soil mechanics [12,13] and represent a very active area of research. An extensive review on the subject is beyond the scope of the present work.

In the 1980s, the applied mechanics community built on the resemblance with molecular gases and developed a kinetic theory for granular gases [14–18], in which the stresses originated from momentum exchange in, for the sake of simplicity, binary, instantaneous, uncorrelated collisions between identical, frictionless, rigid spheres or disks. The same mechanism of momentum exchange at the origin of the granular stresses was first identified by Bagnold [4] in his description of the inertial regime. Unlike Bagnold, however, the kinetic theory of granular gases introduced a measure of the intensity of the particle velocity fluctuations, the so-called granular temperature, as an additional hydrodynamic field. The dissipation of the kinetic energy associated with the velocity fluctuations into true thermal heat through the inelasticity of collisions [16] is the key distinction between molecular and granular gases [1].

Initially limited to slightly inelastic, frictionless particles, the kinetic theory of granular gases was later expanded to account for frictional [19–22] and inelastic collisions [23]. Anisotropic distributions of the velocity fluctuations [1,24–28] have also been accounted for, and have been shown to be crucial for the explanation of non-Newtonian properties of granular gases such as differences in the normal stresses. The evidence [29,30] that, at solid volume fraction larger than the freezing point, say, 0.49 for spheres [31], velocity correlations develop, leading to phenomenological modifications of the collisional dissipation rate [32–34] that allowed the kinetic theory of granular gases to be successfully applied to very dense flows, up to about 0.6 in volume fraction [35–37]. Finally, extensions to finite duration of the collisions [38,39] and nonspherical shapes [40,41] have also been proposed.

Unfortunately, it is still widely believed [42,43] that the kinetic theory of granular gases can only apply to dilute flows of frictionless spheres interacting through binary, instantaneous, and uncorrelated collisions. This original sin motivated the search for a model of granular materials in a hypothetical dense regime, intermediate between the dilute regime of kinetic theory and the quasistatic regime of soil mechanics, in which "grain inertia becomes important but where a contact network still exists that percolates through particles" [44], that is "characterized by enduring contacts between particles" [43], "interacting both by collision and friction" [43]. The result of the collective effort by the French community of scientists involved in granular physics was the well-known inertial rheology [44,45]. In its simplest form, this is a phenomenological, algebraic relation between the ratio of the shear to the normal stress and a dimensionless measure of the particle shear rate, the so-called inertial number, that can be employed to determine the flow field in incompressible, dense granular flows once the distributions of the stresses are known. Another phenomenological, algebraic relation between the solid volume fraction and the inertial number permits to deal with compressibility [46]. The simplicity of the inertial rheology, especially in comparison with the seemingly discouraging complications of kinetic theory, with its heavy usage of statistical mechanics, integro-differential equations, and somewhat cumbersome notation, determined its widespread popularity, with applications, to cite a few, ranging from column collapse [47] to unsteady shearing flows [48], sediment transport [49,50], segregation [51], suspensions [52,53], and flows of nonspherical particles [54].

As already pointed out in one of the first papers that introduced the inertial rheology [46], the latter is simply a rearrangement of Bagnold's rheology in his inertial regime [4] and, therefore, suffers from the same drawback: it ignores the role of the particle velocity fluctuations and the kinetic energy associated with them. Especially in the last 15 years or so, a number of experiments and discrete numerical simulations have been carried out and indeed proved the failure of the inertial rheology in heterogeneous flows [11,55,56], that is, flows in which the solid volume fraction is not uniformly or almost uniformly distributed in the domain.

As a result, the inertial rheology has been amended to deal with heterogeneities by either introducing a Laplacian term in the inertial number directly in the expression for the shear-to-normal stress ratio [57,58] or proposing a new hydrodynamic field, the granular fluidity, and the corresponding balance equation that also contains a Laplacian term [56,59,60]. These so-called

nonlocal models—nonlocality originating from the Laplacian terms—have gained a lot of attention, because they are able to overcome the weaknesses of the inertial rheology while maintaining the framework that has become so familiar to a plethora of researchers in the field. In so doing, however, they have lost much of the simplicity of the original, local inertial rheology: algebraic relations have been replaced by differential equations, and boundary conditions of unclear physical meaning on the inertial number or the granular fluidity and their derivatives must be provided. The degree of complication in nonlocal models is similar to that of kinetic theories of granular gases, without the clear link between the microscopic properties of the particles and the macroscopic stresses provided by the latter.

Here, despite the fact that the kinetic theory of granular gases has been naturally derived for three-dimensional (3D) flows, and that 3D extensions of the local and nonlocal inertial rheology have been proposed [61,62], the focus is, for simplicity, on unidirectional, shearing flows of identical spheres. Polydispersity [63] and/or asphericity [64] are not expected to alter the qualitative features of such flows.

First, already published but scattered results will permit the clarification of some inaccurate, yet abundant, statements about the mechanisms at the origin of the stresses in dense granular flows of realistic particles, such as the frictional-collisional duality, and the presence of long-lasting, multiple contacts forming a network.

Then, despite being already pointed out in a number of papers [34,65], the local inertial rheology will be explicitly deduced from the kinetic theory of granular gases in the special case of steady, homogeneous flows. This allows the determination of the coefficients in the inertial rheology from the microscopic properties of the particles.

Finally, following a few hints [66,67] that already pointed at some common ground, the balance equation of the granular fluidity will be derived from the balance of fluctuation kinetic energy of granular gases, to complete a (re)unification of the only two current candidates for a universal theory of granular flows.

II. FROM MICROSCOPIC INTERACTIONS TO MACROSCOPIC STRESSES

Identical, cohesionless spheres of diameter d and mass density ρ_p are unidirectionally sheared in the presence or in the absence of a gravitational field, g being the gravitational acceleration. The hydrodynamic fields are the solid volume fraction ν, the component of the mean particle velocity in the flow direction, u, and the granular temperature, T, one-third of the mean square of the fluctuations in the particle translational velocity. The derivative of u in the direction perpendicular to the flow is the shear rate, $\dot{\gamma}$. Ignoring the anisotropy in the normal stresses, significant especially in dilute conditions [27], the only nonzero elements of the stress tensor are, then, the pressure p and the shear stress s. For simplicity, the particle mean spin and the strength of the fluctuations in the angular velocity (the rotational temperature) are not considered as additional hydrodynamic fields, even if this should be the most rigorous approach for frictional particles [20].

A. Hard spheres: Always rate dependent

Let us first focus on the limit case of hard, that is, infinitely rigid, spheres, which is the paradigm on which kinetic theories are built. For purely repulsive hard spheres, the contact duration is zero by definition, and there is, therefore, zero probability that more than two particles are in contact at the same time: hard spheres only interact through binary, instantaneous collisions. The collision is characterized by the change in the velocity experienced by the particles before and after the contact. Naturally, the momentum of the system composed of the two particles is conserved, but the single particles can exchange momentum. Figure 1 shows the most general situation in which two spheres, labeled 1 and 2, possess translational velocities $\mathbf{c}_1$ and $\mathbf{c}_2$ and angular velocities $\boldsymbol{\omega}_1$ and $\boldsymbol{\omega}_2$ prior to collision that change into $\mathbf{c}_1'$, $\mathbf{c}_2'$, $\boldsymbol{\omega}_1'$, and $\boldsymbol{\omega}_2'$ afterward. The unit vector $\mathbf{k}$ is directed from the center of particle 1 to the center of particle 2. The change in the particle velocities due to the collision

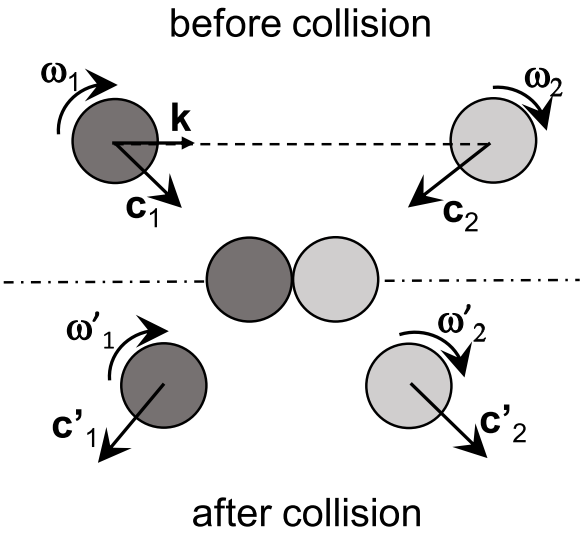

FIG. 1. Sketch of the collisional encounter between two hard spheres.

is proportional to the impulse of the force exerted on particle 1 by particle 2 [21]. The simplest but still realistic model for the impulse [68,69] involves three dimensionless constants, namely, the coefficients of normal, e_n, and tangential, e_t, restitution and the coefficient of sliding friction, μ. The coefficients of restitution are the negative of the ratios of the normal and tangential components of the relative velocity of the points of contact (so that $e_n, e_t \leqslant 1$; collisions are perfectly elastic when they are equal to one), while the coefficient of sliding friction originates from Coulomb's law and relates the tangential to the normal component of the impulse when sliding occurs ($\mu \geqslant 0$; frictionless particles have $\mu = 0$). Indeed, collisions can be sticking if the tangent of the angle between $\mathbf{k}$ and the relative velocity of the contact points is less than a critical value, given by $7\mu(1 + e_n)/[2(1 + e_t)]$, and sliding otherwise [21]. Sticking collisions only depend on e_n and e_t, while sliding collisions depend on e_n and μ. These three coefficients can be measured in experiments [70] and are microscopic inputs of most of the numerical simulations based on the discrete element method (DEM) [71].

Kinetic theories make use of statistical mechanics to perform averaging and obtain a continuum, hydrodynamic description of granular gases. This averaging involves the single-particle velocity distribution function that describes the probability that a particle possesses a certain velocity at a certain location and at a certain time. To describe the change in quantities associated with the binary collisions, one should use the two-particle velocity distribution function of the two colliding spheres. In the absence of velocity correlations (molecular chaos) [72], and for particles of finite size, kinetic theories adopt the Enskog approximation [20], so that the two-particle velocity distribution is taken to be equal to the product of the two single-particle velocity distribution functions times a factor χ_0. The latter is the radial distribution function at contact, a function of the solid volume fraction, that accounts for excluded volume and hindrance [72]. Although in principle χ_0 can be directly measured in, e.g., numerical simulations [30], it is more commonly fitted to match the measurements of, e.g., the stresses [30,36]. For instance, by fitting the dependence of the pressure on the solid volume fraction in steady, heterogeneous shearing flows of frictionless spheres between rigid, bumpy planes [36], later extended and tested against DEM simulations of steady, homogeneous flows of frictional spheres [65], the following expression has been proposed:

$$\chi_0 = \left[\mathrm{H}(\nu - 0.4)\left(\frac{\nu - 0.4}{\nu_c - 0.4}\right)^2\right]\frac{2 - \nu}{2(1 - \nu)^3} + \mathrm{H}(\nu - 0.4)\left(\frac{\nu - 0.4}{\nu_c - 0.4}\right)^2\frac{2}{\nu_c - \nu}. \tag{1}$$

In Eq. (1), H(·) is the Heaviside function. Equation (1) is similar to the expression first proposed by Torquato [31], but limited to nearly elastic spheres ($e_n \approx 1$), in that it recovers the well-known Carnahan-Starling radial distribution function at contact [73] at small solid volume fractions and is singular at a maximum value of the solid volume fraction less than unity. Unlike Torquato's expression, however, Eq. (1) shows a superior agreement with the discrete simulations if $e_n \leqslant 0.95$ [36] and has the advantage that the derivative of χ_0 with respect to ν is continuous over the entire range of admissible solid volume fraction, thus facilitating the numerical solution of the differential equations governing granular flows [74]. The radial distribution function tends to unity for $\nu \to 0$, and is inversely proportional to $\nu_c - \nu$ for $\nu \to \nu_c$ [36], where ν_c is a critical volume fraction. The singularity of χ_0 at ν_c implies that random assemblies of hard spheres are forbidden at volume fractions larger than the critical—larger volume fractions are accessible if crystallization occurs [25]. DEM simulations [65] have shown that ν_c is a decreasing function of the friction coefficient, μ (see later).

Now, repeating Maxwell's arguments [72], one can imagine spheres having an ensemble-averaged velocity field, u, in one particular direction, and random fluctuations around it, of magnitude equal to the square root of the granular temperature. With the particle diameter, d, providing the only length scale of the system, the collision frequency must be proportional to $T^{1/2}/d$. The inverse of the collision frequency is the time of free flight, t_f, i.e., the time that on average a particle spends without interacting with other particles. The collision frequency is also the rate at which particles cross a certain surface, thus carrying momentum and kinetic energy with them. The transport of momentum across a surface is precisely the physical mechanism at the origin of the so-called streaming (or kinetic) components of the granular stresses. Momentum and kinetic energy can also cross a surface through the collisional exchange between two spheres whose centers lie on opposite sides of the surface. This second mechanism gives rise to the collisional components of the stresses [16]. On average, the particles have $mT^{1/2}$ momentum in the direction perpendicular to the flow, and $md\dot{\gamma}$ in the direction parallel to the flow, where $m = \pi \rho_p d^3/6$ is the mass of a sphere. Pressure and shear stress are the rate of exchange of momentum perpendicular and parallel to the flow, respectively, per unit surface area (proportional to d^2). Then, it must be $p \propto \rho_p d^3 T^{1/2} T^{1/2}/d/d^2 = \rho_p T$ and $s \propto \rho_p d^3 d\dot{\gamma} T^{1/2}/d/d^2 = \rho_p d T^{1/2} \dot{\gamma}$. These are the kinetic theory scaling laws and show that stresses are inertial, because they are proportional to the particle mass density, and rate dependent, through the shear rate and the frequency of collisions (see later).

Deriving the scaling is easy, but obtaining the full expressions for the stresses requires lots of calculations [20,23] with perturbations in terms of small parameters involving the spatial gradients [72] and the coefficients of restitution [16]. Then, there are different versions of the kinetic theory, depending on the highest order retained in the perturbations. In, perhaps, the simplest kinetic theory able to capture most of the physics of granular gases composed of realistic, frictional particles [21], the constitutive relations for the stresses are

$$p = \rho_p \nu [1 + 2(1 + e_n)\nu \chi_0] T, \tag{2}$$

and

$$s = \rho_p \frac{8 J \nu^2 \chi_0}{5\pi^{1/2}} d T^{1/2} \dot{\gamma}, \tag{3}$$

where

$$J = \left\{ \frac{1 + e_n}{2} + \frac{\pi}{32} \frac{[5 + 2(1 + e_n)(3e_n - 1)\nu\chi_0][5 + 4(1 + e_n)\nu\chi_0]}{\left[24 - 6(1 - e_n)^2 - 5\left(1 - e_n^2\right)\right]\nu^2 \chi_0^2} \right\} \left[1 + \frac{\pi}{12} \frac{5 - 3(2 - e_n)}{3 - e_n} \right]. \tag{4}$$

The term between curly brackets coincides with the expression reported in Ref. [36], based on the calculations of Ref. [23], a kinetic theory that does not account for the anisotropy in the

single-particle velocity distribution function [24]. The factor between square brackets has been determined in Ref. [27] as the lowest-order correction to the shear stress that captures this anisotropy.

Given that the stresses depend on the granular temperature, a balance for the kinetic energy associated with the fluctuations in the translational velocity is required. In unidirectional flows, the balance is

$$\frac{3}{2}\rho_p \nu \frac{\mathrm{d}T}{\mathrm{d}t} = -\nabla \cdot \mathbf{Q} + s\dot{\gamma} - \Gamma, \tag{5}$$

where the term on the left-hand side represents the rate of change of the fluctuation kinetic energy; the first term on the right-hand side is the diffusion of fluctuation kinetic energy through the particle agitation, with $\mathbf{Q}$ the flux of kinetic energy (actually, in unidirectional flows, it should be $\nabla \cdot \mathbf{Q} = \partial_y Q_y$); the second term on the right-hand side is the production of fluctuation energy through the work of the shear stress; and the last term on the right-hand side, Γ, is the rate of dissipation of the fluctuation energy. This energy balance relates the granular temperature to the shear rate; hence, as anticipated, the collision frequency and the pressure for hard spheres are always rate dependent.

The energy flux can be written as

$$\mathbf{Q} = -\rho_p \frac{4M\nu^2\chi_0}{\pi^{1/2}} d T^{1/2} \nabla T - \rho_p \frac{25\pi^{1/2} N}{128\nu} d T^{3/2} \nabla \nu, \tag{6}$$

where [36]

$$M = \frac{1+e_n}{2} + \frac{9\pi}{144} \frac{[5+3(1+e_n)^2(2e_n-1)\nu\chi_0][5+6(1+e_n)\nu\chi_0]}{\left[16(1+e_n) - 7\left(1-e_n^2\right)\right]\nu^2\chi_0^2}, \tag{7}$$

based on the calculations of Ref. [23]. The analytical expression for the coefficient $N = N(e_n, \nu, \chi_0)$ can be found in Ref. [36].

The rate of dissipation, Γ, includes the direct dissipation of kinetic energy through the inelasticity of the collisions and, for frictional spheres, an exchange term, eventually also dissipated, between the kinetic energy associated with fluctuations in translational velocity and the kinetic energy associated with fluctuations in rotational velocity [20]. It has been shown [21,75] that, at least in homogeneous shearing flows, the exchange term is proportional to the rate of collisional dissipation through a function of the coefficients of restitution and friction. Hence, Γ has the following expression [21,33]:

$$\Gamma = \rho_p \frac{12\left(1-e_{\mathrm{eff}}^2\right)\nu^2\chi_0}{\pi^{1/2}} \frac{T^{3/2}}{L}, \tag{8}$$

where $e_{\mathrm{eff}} = e_{\mathrm{eff}}(e_n, e_t, \mu)$ is an effective coefficient of restitution [22] that accounts for the additional pseudodissipation of translational fluctuation energy into rotational fluctuation energy. The expression for the effective coefficient of restitution in the limit of nearly elastic particles was analytically derived in Ref. [21] as $e_{\mathrm{eff}} = e_n - (\pi/2)\mu + (9/2)\mu^2$. A more general but implicit expression, so that e_{eff} must be determined numerically, was obtained in Ref. [22]. The quantity L in Eq. (8) is the correlation length [32,33], a phenomenological quantity introduced to account for the reduction in the rate of dissipation due to correlations in particle velocity fluctuations (breaking of the molecular chaos assumption) observed in discrete numerical simulations at volume fractions larger than 0.49 [30]. The correlation length could be directly measured in numerical simulations [76]. However, its expression has been obtained through indirect fitting of the dependence of the granular temperature on the solid volume fraction in homogeneous shearing flows [77], and reads

$$\frac{L}{d} = \left[\frac{2J}{15\left(1-e_{\mathrm{eff}}^2\right)}\right]^{1/2} \left[1 + \frac{26(1-e_{\mathrm{eff}})}{15} \frac{\mathrm{H}(\nu-0.49)(\nu-0.49)}{0.64-\nu}\right]^{3/2} \frac{d\dot{\gamma}}{T^{1/2}}, \tag{9}$$

where 0.64 is the value of the solid volume fraction at random close packing for spheres [31]. Direct measurements of the correlation length in different flow configurations would permit a more

thorough assessment of the general validity of Eq. (9). However, it is striking that is has been shown to hold even in steady, homogeneous shearing flows of cylinders [41]. Crucially, Eq. (9) indicates that the correlation length is singular at the random close packing, while the stresses, proportional to the radial distribution function at contact [Eqs. (2) and (3)], are singular at ν_c [65].

B. Soft spheres: Rate-dependent and rate-independent stresses

Real particles are not infinitely rigid and deform when interacting. Simple contact models are used in DEM simulations to reproduce the dynamics of the interaction between soft spheres. In most of these simulations, the particles retain their spherical shape, and the deformation is replaced with overlapping volumes. Elastic springs, viscous dashpots, and sliders normal and tangential to the plane of contact are, then, employed to translate the overlap into dissipative, repulsive forces between the particles [71]. This simple contact model permits to understand the different physics that arises because of the finite particle stiffness, quantified through the stiffness of the elastic spring in the direction normal to the contact, k_n. The stiffness of the spring in the tangential direction is usually taken to be proportional to k_n, so that the latter is the only additional microscopic parameter that is necessary to characterize, at the microscopic level, the soft particles (it can be shown that setting the properties of the viscous dashpots is equivalent to imposing the values of the coefficients of restitution). A graphical summary of the differences between the interaction of hard and soft spheres is shown in Fig. 2. Hard spheres do not overlap, impulses with associated momentum exchanges are generated at instantaneous contacts, and the average time between two successive impulses or collisions is the time of free flight, t_f.

For soft spheres, the contact duration, t_c, is nonzero, and decreases with k_n. In that time, the overlap grows, reaches a peak, and then decreases, and so does the repulsive force between the spheres, that is an increasing function of the overlap. If the solid volume fraction is less than the critical, then the distance between the edges of the nearest spheres is, on average, larger than zero. Hence, in between two successive contacts, the particles follow a nonzero mean free path in a nonzero time t_f (Fig. 2). It has been proposed [38,39] to substitute the collision frequency in the constitutive relations of kinetic theory of hard spheres with the inverse of $t_f + t_c$ to model the collisional behavior of soft spheres. This modification accounts for the finite duration of the contacts, while still assuming only binary interactions, although the probability of multiple contacts increases with the contact duration [78,79]. However, the notable agreement, shown in Ref. [39], between the stresses predicted by the theory and the measurements [80] in DEM simulations of steady, homogeneous flows [Fig. 3(a)], over a range of 11 orders of magnitude in the particle stiffness, indicate that multiple contacts only play a minor role. Given that t_f vanishes at the critical volume fraction, but t_c remains finite there, the finite stiffness of the particles also permits to regularize the stresses and remove their singularity at ν_c.

Indeed, unlike hard spheres, random assemblies of soft spheres at solid volume fraction larger than the critical are possible, because they can overlap. If the solid volume fraction is larger than the critical, the average distance between the centers of the nearest spheres is less than one diameter. Hence, there is an average nonzero overlap between adjacent spheres. On top of this, particles still fluctuate, breaking and reforming contacts under shearing flow conditions. The picture is that of a network of permanently compressed elastic springs that is constantly rearranging. Phases, of average duration t_c, of overlap growing, reaching a peak, and decreasing associated with momentum exchange (collisions) can still be identified on top of a ground state of permanent repulsive forces associated with the residual overlap (Fig. 2). The latter is at the origin of rate-independent components of the stresses, proportional to the particle stiffness, superimposed upon inertial, rate-dependent components of the stresses still due to collisional interactions, with the collision frequency set by $1/t_c$. For sufficiently rigid particles, the rate-independent contributions dominate [39]. The rate-independent components of the stresses have been termed elastic [39,81], because of the proportionality to the particle stiffness.

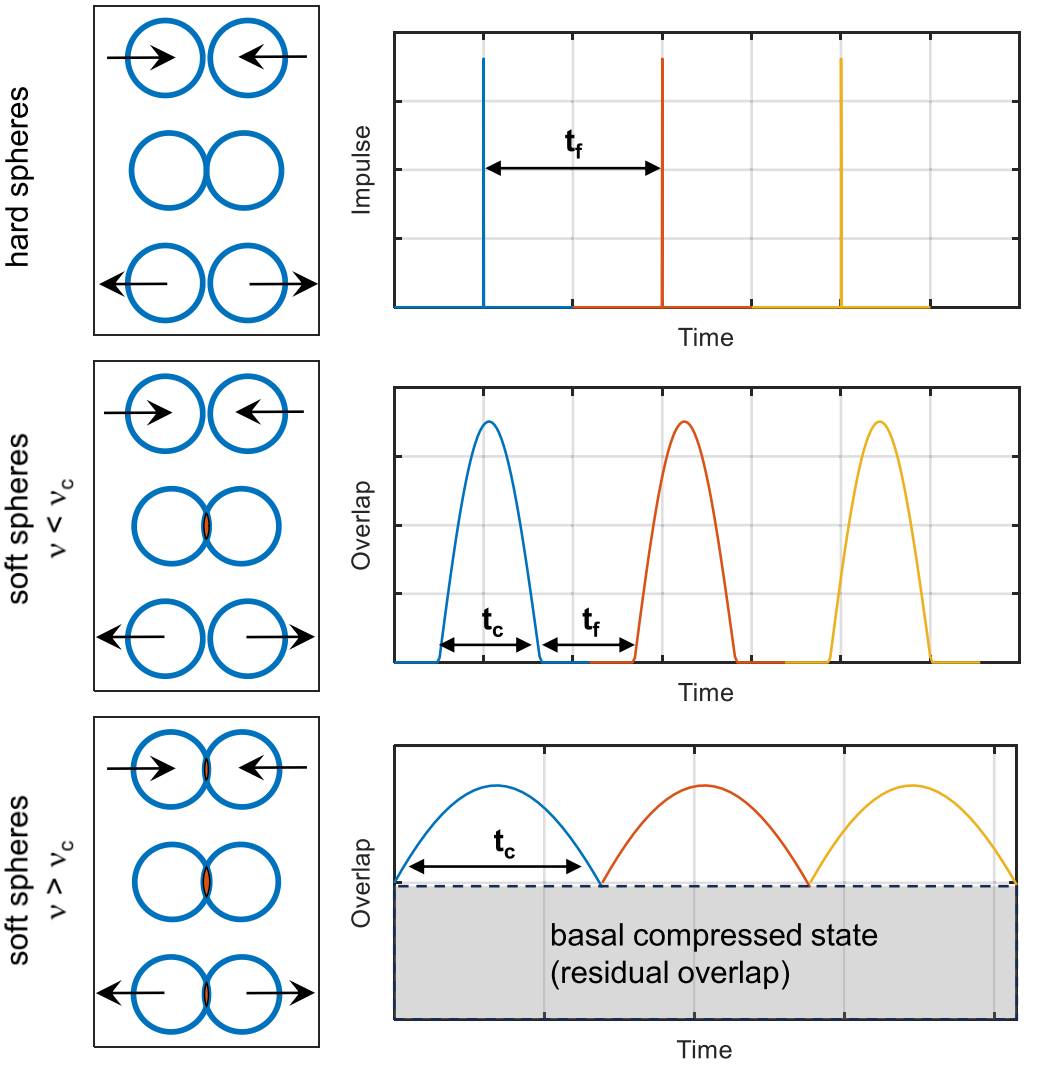

FIG. 2. Schematics of a single interaction between two spheres (on the left, the overlap area is indicated in orange) and corresponding time sequence of impulse or overlap for three such events (on the right) for (from top to bottom) hard spheres, soft spheres at subcritical volume fraction, and soft spheres at supercritical volume fraction. Also shown are the time of free flight and the finite duration of the interaction.

Based on the above-mentioned findings on the physics of flows of hard and soft spheres, granular flows are *inertial* or, equivalently, *collisional* if $\nu < \nu_c$ (subcritical). If $\nu \geqslant \nu_c$ (supercritical), and the rate-independent components of the stresses dominate, granular flows are in the *quasistatic* regime. Then, the determination of the critical solid volume fraction and its dependence on the microscopic properties of the particles is crucial in modeling granular flows.

C. Critical point

The critical point marks the transition from a purely rate-dependent to a mix of rate-dependent and rate-independent behavior. So far, this critical point has been characterized in terms of a

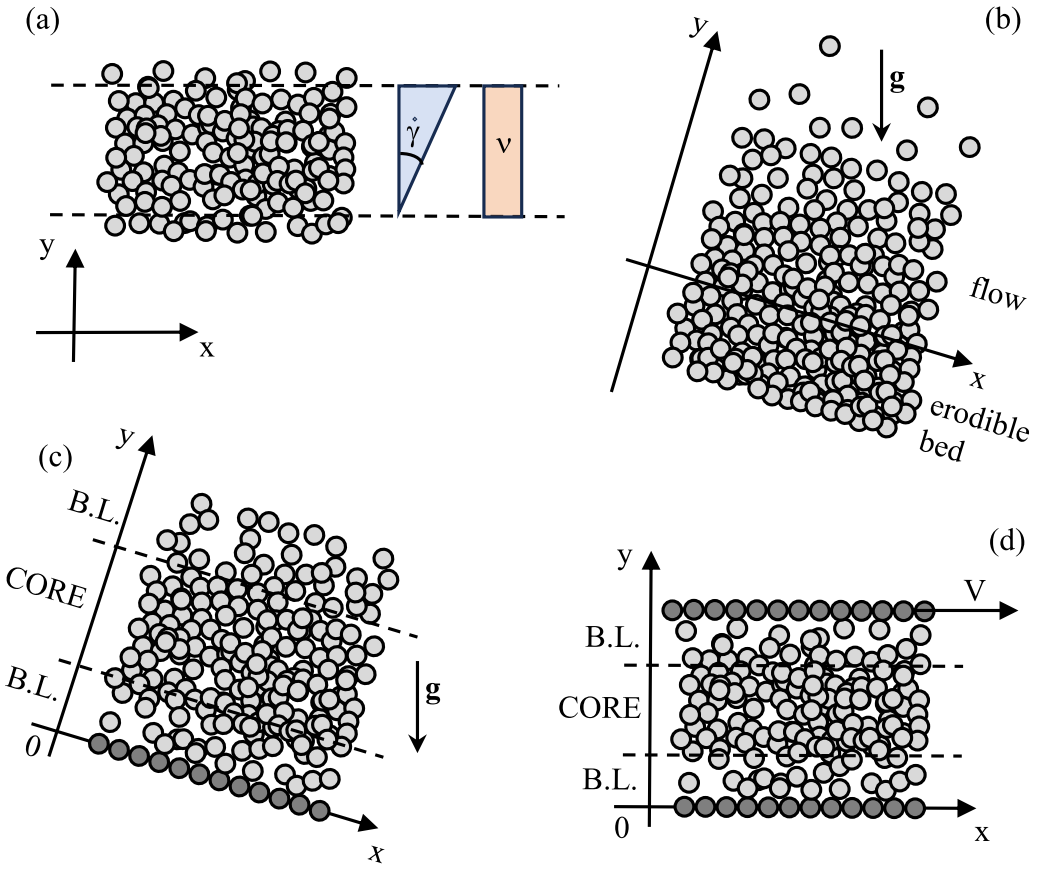

FIG. 3. Unidirectional flow configurations with the frame of reference: (a) steady, homogeneous (simple) shearing with linear distribution of the mean velocity and uniform distribution of the solid volume fraction; steady, gravity-driven, heterogeneous flow over (b) an erodible bed with lateral confinement and (c) a rigid, bumpy bed without lateral confinement; (d) steady, heterogeneous flow between parallel, rigid, bumpy plates in relative motion (Couette flow) in the absence of gravity. In (c) and (d), the core region, in which the solid volume fraction is uniform, is sandwiched between two conductive boundary layers (B.L.).

particular value of the solid volume fraction, ν_c. However, measurements [79] in DEM simulations of steady, homogeneous flows [Fig. 3(a)] of soft spheres show a monotonically increasing relation between the solid volume fraction and the coordination number, Z, the average number of contacts per particle. Thus, there is also a critical coordination number, Z_c. Four different methods have been proposed in the literature to identify the coordinates $\{\nu_c, Z_c\}$ of the critical point:

(i) In DEM simulations of steady, homogeneous, shearing flows (also called simple shearing) carried out in a periodic cell of fixed volume [Fig. 3(a)], one can adjust the number of particles in the cell to obtain a particular value of the solid volume fraction. For a given set of the particle contact properties (e_n, e_t, μ, and k_n) and the shear rate, $\dot{\gamma}$, the average pressure and shear stress can, then, be measured. The ratio of the contact time, $t_c = d^{3/2}/\sqrt{k_n/\rho_p}$ [82], over the timescale associated with the shearing flow, $1/\dot{\gamma}$, is a dimensionless shear rate that quantifies the influence of the particle stiffness on the collisions, for subcritical flows, and the influence of the rate-dependent components of the stresses, for supercritical flows. As shown in Fig. 4(a) for the particular case of frictional spheres with $\mu = 0.5$, changing the dimensionless shear rate at two slightly different values of the solid volume fraction, 0.584 and 0.594, permits to identify a bifurcation in the behavior of the dimensionless pressure, pd/k_n [80]. At the lowest values of the dimensionless shear rate, the

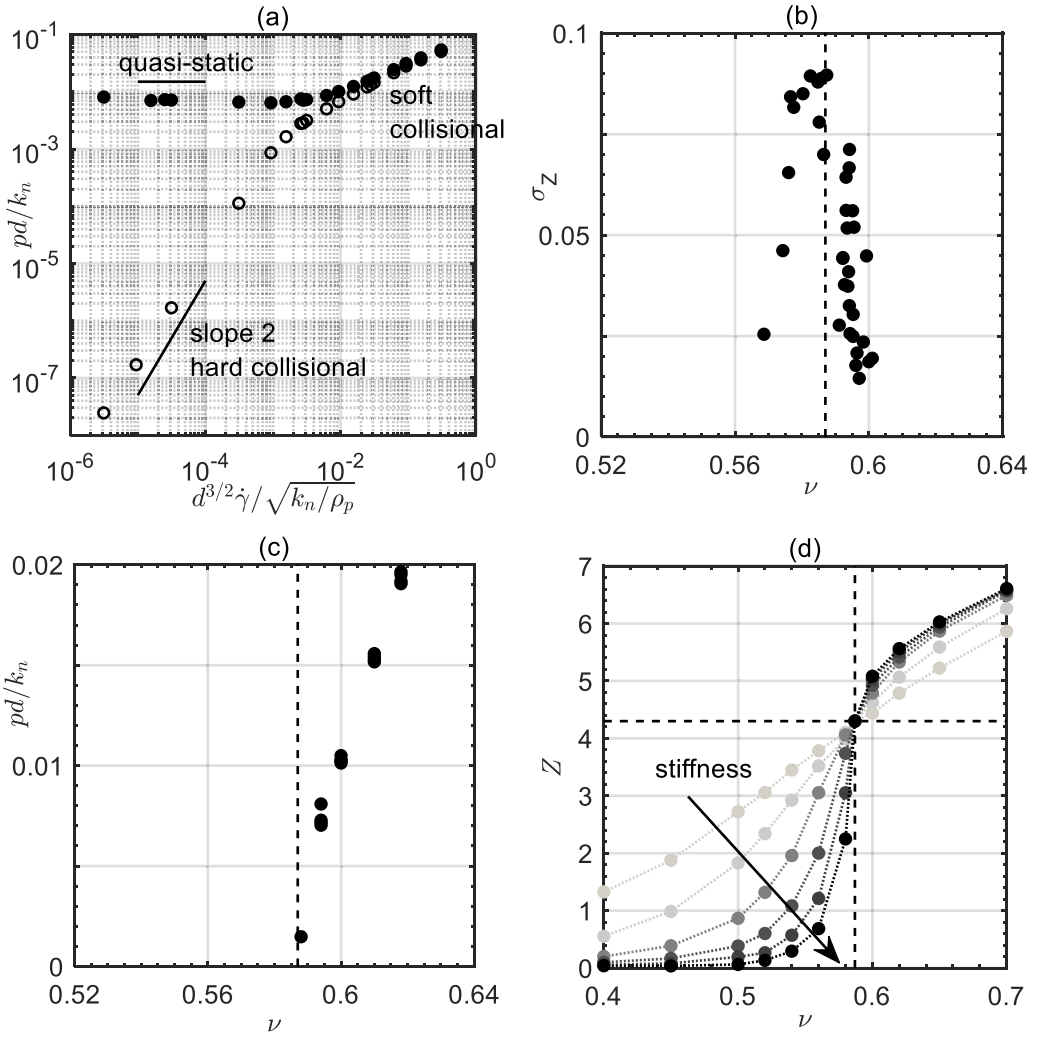

FIG. 4. (a) Dimensionless pressure as a function of the dimensionless shear rate measured in DEM simulations [80] of volume-controlled, steady, homogeneous shearing flows of spheres with $e_n = 0.7$, $e_t = 1$, and $\mu = 0.5$, at $\nu = 0.594$ (solid circles) and $\nu = 0.584$ (open circles). (b) Magnitude of the fluctuations in the coordination number as a function of the solid volume fraction measured in DEM simulations [82] of steady, heterogeneous, gravity-driven flows of spheres with $e_n = 0.88$, $e_t = 1$, $\mu = 0.5$, and $k_n \approx 3\times10^6 \rho_p g d^2$. (c) Same as in (a), but the dimensionless pressure is plotted as a function of the solid volume fraction (only data in the quasistatic limit are shown). (d) Coordination number as a function of the solid volume fraction measured in DEM simulations [79] of volume-controlled, steady, homogeneous shearing flows of spheres with $e_n = 0.7$, $e_t = 1$, and $\mu = 0.5$, for different values of the dimensionless stiffness, $k_n/(\rho_p d^3 \dot{\gamma}^2)$, ranging from 10^2 (light gray circles) to 10^7 (black circles). In all plots, the dashed lines represent the coordinates of the critical point for $\mu = 0.5$.

dimensionless pressure is either rate independent (quasistatic regime) at $\nu = 0.594$ or grows as the square of the shear rate (collisional regime for hard spheres, see later) at $\nu = 0.584$. Then, ν_c must lie somewhere between 0.584 and 0.594. At the largest values of the dimensionless shear rate, regardless of being subcritical or supercritical, the pressure is rate dependent, but the exponent in the power law is less than 2. In this regime, the granular assembly can be imagined as composed of agitated, squishy spheres that exchange momentum in collisions (soft collisional regime).

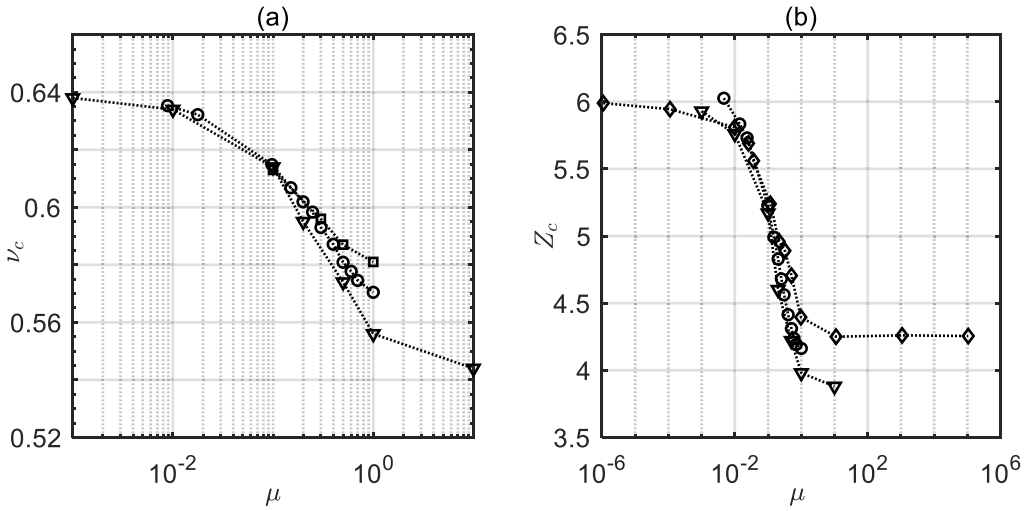

FIG. 5. Measured critical (a) solid volume fraction and (b) coordination number as functions of the friction coefficient as reported in Ref. [85] (circles), Ref. [84] (triangles), Ref. [80] (squares), and Ref. [83] (diamonds).

(ii) Even under steady conditions, measurements in DEM simulations reveal fluctuations in time. The magnitude of the fluctuations of the coordination number in steady, homogeneous [simple shearing, Fig. 3(a)] [80] and heterogeneous [gravity-driven, inclined flows over erodible beds, Fig. 3(b)] [74] flows reaches a peak at the critical solid volume fraction [Fig. 4(b)]. The peak is likely associated with the fact that the contact network is unstable at the critical point, and intermittently builds up and disappears. Although it has not been proven yet, it is likely that the stiffer the particles, the more pronounced would be the peak in the fluctuations.

(iii) A third method that has been used in static [83,84] and quasistatic [85] conditions consists in determining the values of the solid volume fraction and the coordination number at which the pressure, originating from the elastic contacts between the particles, vanishes (jamming point) [2]. This is obtained by extrapolating to zero the dependence of the rate-independent component of p on ν and Z [Fig. 4(c)].

(iv) Finally, as mentioned, the coordination number and the solid volume fraction are in a one-to-one relation under steady and homogeneous conditions. In simple shearing, this curve depends on the dimensionless shear rate $d^{3/2}\dot{\gamma}/\sqrt{k_n/\rho_p}$ [79,86]. At the critical point, the average distance between the edges of adjacent spheres is zero, and the average overlap is also zero: the stiffness plays no role. Then, the above-mentioned curves, $Z = Z(\nu)$, must intersect there [Fig. 4(d)]. This method has been employed to determine the coordinates of the critical point also for cylinders [87].

Figure 5 shows that the coordinates of the critical point measured by various authors using the above-mentioned methods only depend on the friction coefficient. Some discrepancies between the measurements can be spotted for extremely frictional spheres, but the data nicely collapse for any realistic values of μ (say, up to 0.5, as determined in physical experiments [70] on colliding particles).

It is worth emphasizing that, in the more general case of unsteady and/or heterogeneous flows, the solid volume fraction and the coordination number uncouple. It has been shown that rate-independent components of the stresses arise: only for $\nu \geqslant \nu_c$ and $Z \geqslant Z_c$ for unsteady, homogeneous flows [88], while even for $\nu \geqslant \nu_c$ and $Z < Z_c$ for steady, heterogeneous flows [82].

As a final remark, even if a more realistic Hertzian rather than a linear (Hookean) contact model is employed in the discrete numerical simulations, the plots of, e.g., Fig. 4 remain qualitatively the same. However, different scalings arise, so that, for example, pd/k_n in Fig. 4 must be replaced by $(p_{Hz}/k_{Hz})^{2/3}$, with p_{Hz} the pressure measured using the Hertzian contact model and k_{Hz} the

corresponding normal stiffness [85]. Intuitively, the contact model cannot have any influence on the results when the collisions are nearly instantaneous.

D. The myth of long-lasting, multiple, frictional contacts in dense granular flows

As already mentioned, the kinetic theory was supposed to fail in the presence of long-lasting, multiple, frictional contacts that are allegedly abundant in dense granular flows, "between random loose packing and random close packing" [42]. Random loose and random close packing are now understood as the values of the critical volume fraction ν_c for $\mu \to \infty$ and $\mu = 0$, respectively [84]. Then, on a more rigorous basis, granular flows are dense if ν is between 0.49 and ν_c, that is, in the range where the molecular chaos assumption breaks, but the elastic components of the stresses are still absent.

The idea of long-lasting, multiple contacts in dense granular flows has actually originated from experiments [89] and simulations [90] on quasistatic flows, where the contact duration is much larger than the mean free path, which vanishes, and the coordination number is larger than Z_c (that is, larger than four), indicating multiple contacts.

As explained, the contact duration and the likelihood of multiple contacts are related to the particle stiffness and the rate of shear. For a given value of k_n, at slow shearing, particles at subcritical volume fractions behave as hard grains; that is, collisions are binary and instantaneous [Fig. 4(a)]. In the homogeneous shearing of 1 mm sand (or glass) particles, $\rho_p = 2650\,\mathrm{kg/m^3}$, and Young's modulus, proportional to k_n/d, of order 100 GPa, at 50 Hz, already one order of magnitude larger than typical experimental values [91], $d^{3/2}\dot{\gamma}/\sqrt{k_n/\rho_p} \sim 10^{-7/2}$, well within the hard collisional limit [Fig. 4(a)]. Indeed, at the corresponding dimensionless stiffness $k_n/(\rho_p d^3\dot{\gamma}^2) \sim 10^7$, the coordination number is less than one (binary interactions) up to volume fractions very close to ν_c [Fig. 4(d)]. Even when measured in DEM simulations of gravity-driven, heterogeneous flows over erodible beds [74], relevant for many geophysical applications, the coordination number remains less than one up to solid volume fractions that are 0.02 below the critical value [Fig. 6(a)], although the particle stiffness is three orders of magnitude less than that of sand grains. Figure 6(b) indicates that the pressure measured in DEM simulations of steady, homogeneous flows is independent of the stiffness, and very well captured by the kinetic theory for hard spheres (see next section) for any realistic value of k_n. Departures at solid volume fractions significantly less than the critical can be observed only for extremely soft systems, like 1 mm hydrogel spheres—mass density identical to that of water and Young's modulus of order MPa—sheared at very large rates, say, 50 Hz.

As pointed out in a previous section, the widely believed contrast between collisional and frictional contacts [81,92–96] is indeed fictitious: collisions can be sticking or sliding for frictional particles, or only sliding for frictionless particles. In any case, momentum exchange characterizes the interaction at $\nu \leqslant \nu_c$.

The frictional sliding mechanism at the microscopic level has been invoked to justify the use of a Coulomb-like law to express the elastic component of the shear stress [81,96]. However, at large friction—and unrealistic high values of μ are usually adopted in the numerical simulations to speed up the computations—most of the contacts are sticking, not sliding. More importantly, the elastic stresses are absent in dense granular flows at $\nu \leqslant \nu_c$.

III. STEADY, HOMOGENEOUS FLOWS: BAGNOLD, INERTIAL RHEOLOGY, AND KINETIC THEORY

In Bagnold's seminal work [4] on steady, homogeneous shearing of granular materials under what he called the inertial regime, the author basically repeated Maxwell's arguments [72] that lead to the scalings of kinetic theory for the stresses, but neglecting the role of particle agitation. He assumed that the particle momentum in both the direction parallel and perpendicular to the flow was $md\dot{\gamma}$, and that the frequency of collisions was set by the shear rate, $\dot{\gamma}$. Then, Bagnold obtained $p \propto \rho_p d^3 d\dot{\gamma}\dot{\gamma}/d^2 = \rho_p d^2\dot{\gamma}^2$ and $s \propto p \propto \rho_p d^2\dot{\gamma}^2$. In these expressions, the coefficients

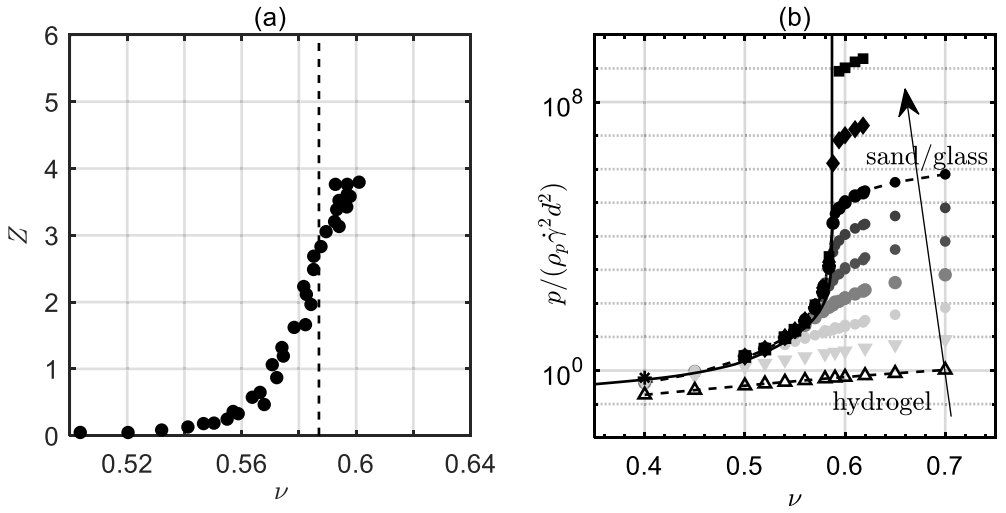

FIG. 6. (a) Coordination number as a function of the solid volume fraction measured in DEM simulations [82] of steady, heterogeneous, gravity-driven flows of spheres with $e_n = 0.88$, $e_t = 1$, $\mu = 0.5$, and $k_n \approx 3\times10^6\rho_p g d^2$. The dashed line indicates the value of ν_c. (b) Dimensionless pressure as a function of the solid volume fraction measured in DEM simulations [80] of volume-controlled, steady, homogeneous shearing flows of spheres with $e_n = 0.7$, $e_t = 1$, and $\mu = 0.5$, at different values of the dimensionless particle stiffness, $k_n/(\rho_p d^3\dot{\gamma}^2)$, ranging from 1 to 10^{11} (the arrow indicates the direction of increasing stiffness). The two dashed lines highlight the data corresponding to 1 mm sand (or glass) and hydrogel spheres sheared at 50 Hz, while the solid line is the prediction of the kinetic theory for hard spheres.

of proportionality are, in general, functions of the solid volume fraction. Obviously, Bagnold's rheology cannot apply in the absence of shearing, nor in situations in which the shear stress vanishes but the pressure does not, as along the midsection of vertical chutes [97].

The inertial rheology [44], proposed 50 years after Bagnold, consists of two phenomenological relations describing, in dense granular flows, the dependence of the solid volume fraction and the stress ratio, $\mu^* = s/p$, on the inertial number, $I = d\dot{\gamma}/\sqrt{p/\rho_p}$. Based on fitting with experimental and numerical measurements, the dependence of the solid volume fraction on the inertial number was taken to be linear [46],

$$\nu = \nu_c - aI, \tag{10}$$

where a is a fitting parameter, and the solid volume fraction at vanishing I is taken to be its critical value ν_c. Actually, in many situations, the dense granular flow is treated as incompressible, and only the dependence of the stress ratio on the inertial number is employed. The most common form of the latter [45] is

$$\mu^* = \mu_c + \frac{\mu_2 - \mu_c}{I_0 + I} I, \tag{11}$$

which implies that the stress ratio tends to its quasistatic, yield value, μ_c, when I vanishes, and asymptotically tends to μ_2 for large I. The coefficients μ_c, μ_2, and I_0 are material dependent and must be empirically determined. Equation (11) is often mistaken as indicating the coexistence of rate-independent and rate-dependent mechanisms at the origin of the shear stress. However, a rate-independent component of the stress ratio does not imply rate-independent stresses. Indeed, Eqs. (10) and (11) can be rephrased as

$$p = \rho_p \frac{a^2}{(\nu_c - \nu)^2} d^2\dot{\gamma}^2, \tag{12}$$

and

$$s = \rho_p \frac{\mu_c a I_0 + \mu_2(\nu_c - \nu)}{a I_0 + \nu_c - \nu} \frac{a^2}{(\nu_c - \nu)^2} d^2 \dot{\gamma}^2, \tag{13}$$

which is exactly Bagnold's rheology, as already recognized [46]. Interestingly, the inertial rheology suggests that both the pressure and the shear stress diverge at the critical volume fraction, but the stress ratio there remains finite.

One of Bagnold's general assumptions was that the "kinetic energy per unit volume of the system is maintained constant by frictional losses" [4]. Despite the only partially correct reference to friction as the source of dissipation, while ignoring the role of inelastic collisions, this is indeed what Eq. (5) shows under steady ($\mathrm{d}T/\mathrm{d}t = 0$) and homogeneous ($\nabla \cdot \mathbf{Q} = 0$) conditions: the fluctuation kinetic energy produced through the work of the shear stress is dissipated through the particle interactions, $s\dot{\gamma} = \Gamma$. The latter, with Eqs. (3), (8), and (9), implies

$$T = \frac{2J}{15\left(1 - e_{\mathrm{eff}}^2\right)} \left[1 + \frac{26(1 - e_{\mathrm{eff}})}{15} \frac{\mathrm{H}(\nu - 0.49)(\nu - 0.49)}{0.64 - \nu}\right] d^2 \dot{\gamma}^2, \tag{14}$$

which is that the granular temperature is proportional to the square of the shear rate and not an independent field. Inserting Eq. (14) into Eqs. (2) and (3) gives

$$p = \rho_p \frac{2J\nu[1 + 2(1 + e_n)\nu\chi_0]}{15\left(1 - e_{\mathrm{eff}}^2\right)} \left[1 + \frac{26(1 - e_{\mathrm{eff}})}{15} \frac{\mathrm{H}(\nu - 0.49)(\nu - 0.49)}{0.64 - \nu}\right] d^2 \dot{\gamma}^2 \tag{15}$$

and

$$s = \rho_p \frac{8J\nu^2\chi_0}{5\pi^{1/2}} \left[\frac{2J}{15\left(1 - e_{\mathrm{eff}}^2\right)}\right]^{1/2} \left[1 + \frac{26(1 - e_{\mathrm{eff}})}{15} \frac{\mathrm{H}(\nu - 0.49)(\nu - 0.49)}{0.64 - \nu}\right]^{1/2} d^2 \dot{\gamma}^2, \tag{16}$$

which is Bagnold's rheology deduced from the kinetic theory. The only parameters in Eqs. (15) and (16), unlike Eqs. (12) and (13), are the microscopic contact coefficients e_n, e_t, and μ. Moreover, Eqs. (15) and (16) are valid over the entire range of solid volume fraction less than the critical, and not only under dense conditions.

For every value of ν, then, Eqs. (15) and (16) permit to calculate the corresponding dimensionless pressure, $p/(\rho_p d^2 \dot{\gamma}^2)$, and dimensionless shear stress, $s/(\rho_p d^2 \dot{\gamma}^2)$. The dimensionless pressure is the inverse of the square of I, and the ratio of the dimensionless shear stress over the dimensionless pressure is μ^*. Hence, the relations $I = I(\nu)$ and $\mu^* = \mu^*(\nu)$, or, equivalently, $\nu = \nu(I)$ and $\mu^* = \mu^*(I)$, can also be deduced from the kinetic theory and plotted against the data.

Figures 7 and 8 show the notable agreement between the predictions of kinetic theory and the results of DEM simulations of steady, homogeneous flows, for different values of the coefficient of normal restitution and friction [80,86,98]. The same measurements of pressure and shear stress are plotted: in the inertial rheology framework, that is with the dimensionless triad $\{\nu, I, \mu^*\}$; using the Bagnold's scaling, that is with the dimensionless triad $\{\nu, p/(\rho_p d^2 \dot{\gamma}^2), s/(\rho_p d^2 \dot{\gamma}^2)\}$; and using the kinetic theory scaling, that is with the dimensionless triad $\{\nu, p/(\rho_p T), s/(\rho_p d T^{1/2} \dot{\gamma})\}$. The solid lines are the predictions of kinetic theory using the three representations—e.g, for Bagnold's and the kinetic theory scalings, Eqs. (15) and (16) or Eqs. (2) and (3) are employed, respectively. The solid volume fraction ranges from 0.2 to its critical value, which is from dilute to very dense conditions. The value of the critical volume fraction is that reported in Ref. [80] for the different friction coefficients, while the expression for χ_0 is that suggested in Ref. [36]. Interestingly, and perhaps counterintuitively, the influence of the coefficient of normal restitution is less evident when the kinetic theory scaling is adopted [Figs. 7(c) and 7(f)]. The DEM simulations reveal a nonmonotonic behavior of the stress ratio with the inertial number [Figs. 7(d) and 8(d)], which is not captured by Eq. (11). The kinetic theory, instead, reproduces the peaks in the stress ratio, which correspond to $\nu = 0.49$, where the correlation in the velocity fluctuations first appears. The

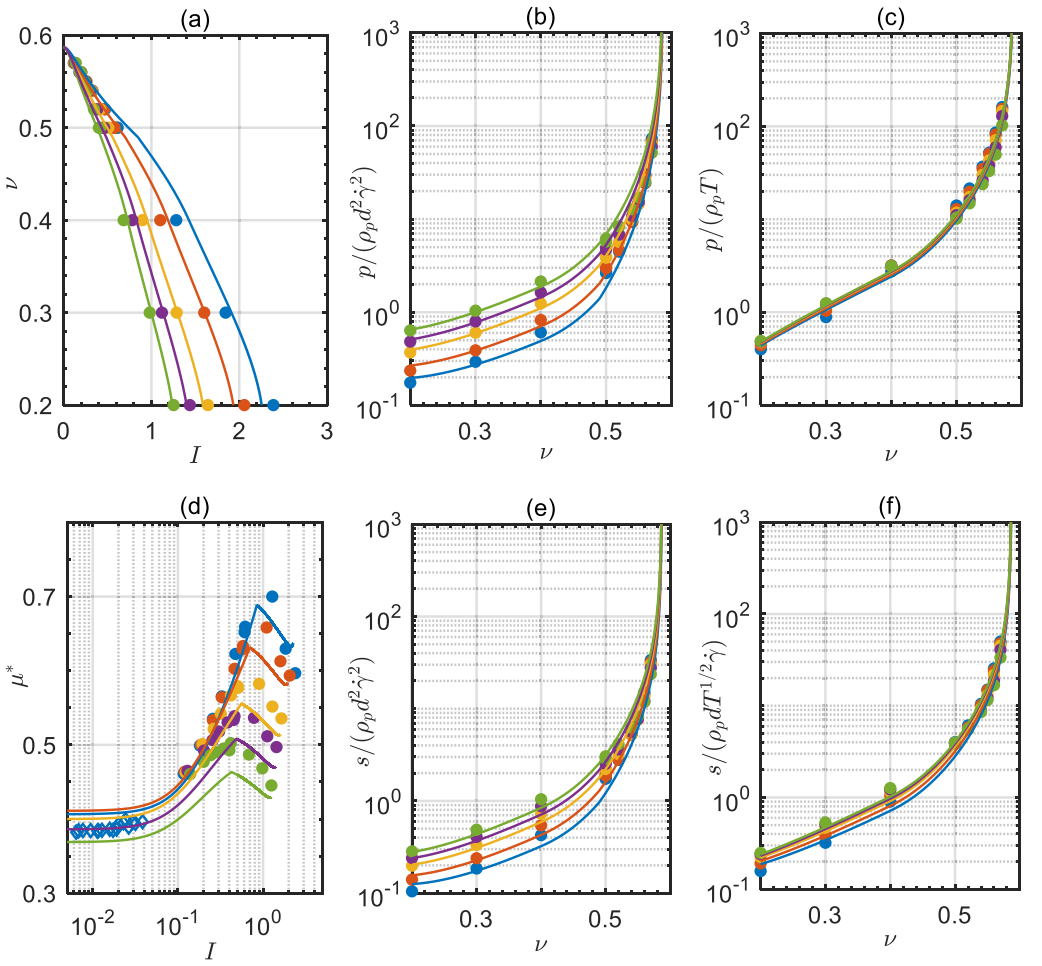

FIG. 7. Measurements (DEM simulations, solid circles) [98] and predictions from kinetic theory (lines) of pressure and shear stress in steady, homogeneous flows at $\nu < \nu_c$ for $e_t = 1$, $\mu = 0.5$, $k_n/(\rho_p d^3\dot{\gamma}^2) > 10^6$ and $e_n = 0.7$ (in blue), $e_n = 0.8$ (in orange), $e_n = 0.9$ (in yellow), $e_n = 0.95$ (in purple), and $e_n = 0.99$ (in green). The data are plotted using [(a) and (d)] the inertial rheology representation, [(b) and (e)] Bagnold's scalings, and [(c) and (f)] the kinetic theory scalings. Also shown in (d) are DEM data [80] for $\nu \geqslant \nu_c$ (open diamonds).

divergence of χ_0 at $\nu = \nu_c$ permits the kinetic theory to capture the singularities [65] in the stresses and their dependence on the coefficient of friction [Figs. 8(b)and 8(c) and Figs. 8(e) and 8(f)].

It is worth noticing that also the kinetic theory, like the inertial rheology, predicts that the stress ratio remains finite at the critical volume fraction, even if the stresses diverge. Indeed, the dense limit, i.e., where $\nu\chi_0 \gg 1$ and

$$J = J_\infty \approx \left[\frac{1+e_n}{2} + \frac{\pi}{4}\frac{(1+e_n)^2(3e_n-1)}{24-6(1-e_n)^2-5\left(1-e_n^2\right)}\right]\left(1+\frac{\pi}{12}\frac{3e_n-1}{3-e_n}\right), \tag{17}$$

of the ratio of Eq. (16) over Eq. (15), evaluated at $\nu = \nu_c$ provides the value of the yield stress ratio,

$$\mu_c = \left[\frac{24J_\infty\left(1-e_{\text{eff}}^2\right)}{5\pi(1+e_n)^2}\right]^{1/2}\left[1+\frac{26(1-e_{\text{eff}})}{15}\frac{\nu_c-0.49}{0.64-\nu_c}\right]^{-1/2}, \tag{18}$$

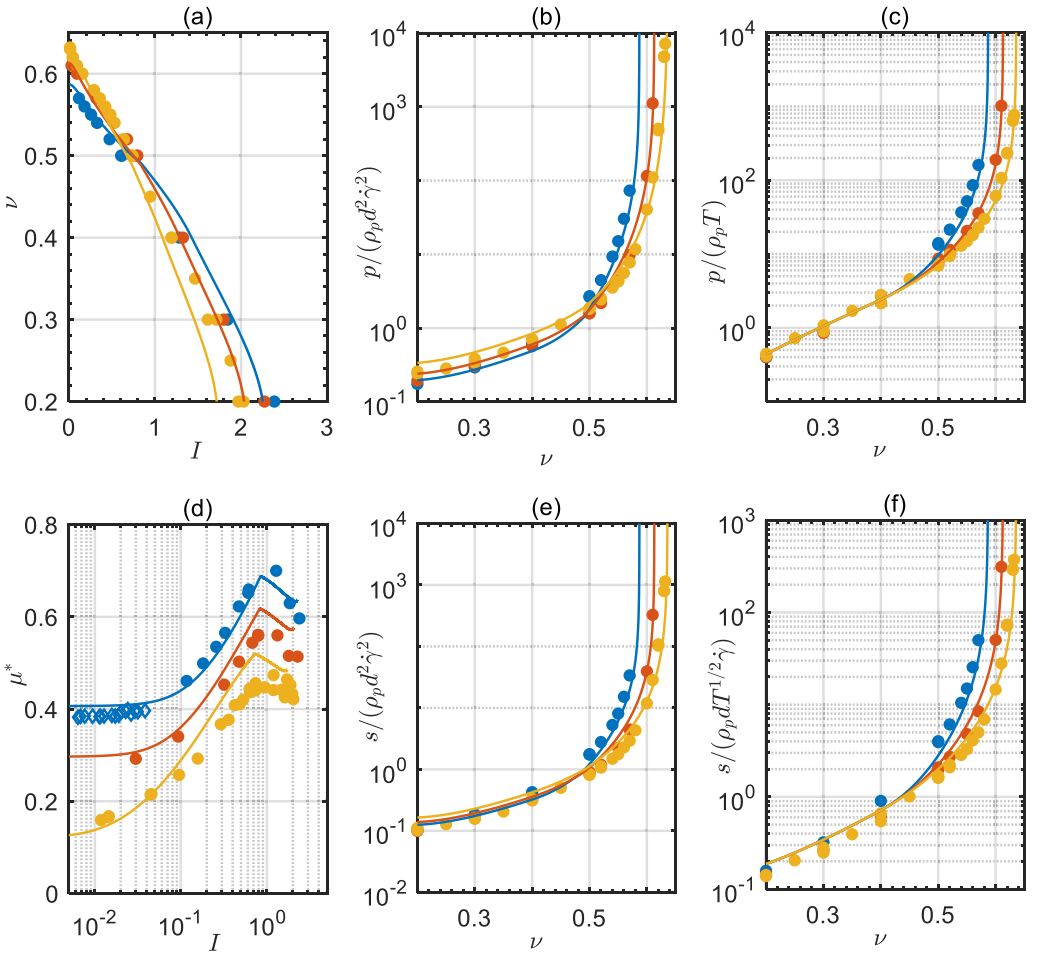

FIG. 8. Measurements (DEM simulations, solid circles) [86,98] and predictions from kinetic theory (lines) of pressure and shear stress in steady, homogeneous flows at $\nu < \nu_c$ for $e_n = 0.7$, $e_t = 1$, $k_n/(\rho_p d^3\dot{\gamma}^2) > 10^6$, and $\mu = 0.5$ (in blue), $\mu = 0.1$ (in orange), and $\mu = 0$ (in yellow). The data are plotted using [(a) and (d)] the inertial rheology representation, [(b) and (e)] Bagnold's scaling, and [(c) and (f)] the kinetic theory scaling. Also shown in (d) are DEM data [80] for $\nu \geqslant \nu_c$ (open diamonds).

as a function of e_n, $e_{\text{eff}} = e_{\text{eff}}(e_n, e_t, \mu)$ [22], and $\nu_c = \nu_c(\mu)$ [Fig. 5(a)]. The agreement between this prediction and the measurements in DEM simulations was shown in Ref. [65] and can be appreciated in Figs. 7(d) and 8(d). The same figures also indicate that Eq. (18), which is the stress ratio of purely rate-dependent stresses at $\nu = \nu_c$, equals the stress ratio of the rate-independent stresses in the quasistatic regime at $\nu > \nu_c$. The physical reason for this is an open question.

One of the advantages of the inertial rheology was that, in many situations, one can conveniently assume incompressibility and only employ Eq. (11), which does not contain information about the solid volume fraction, to solve for dense granular flows, despite some mathematical issues about its ill behavior in certain limits [99]. Due to the strong nonlinear dependence of the stresses on ν, it is not possible, in general, to explicitly express the stress ratio as only a function of the inertial number by manipulating Eqs. (15) and (16). However, if Eq. (11) is a valid approximation of the dependence of the stress ratio on the inertial number for $0.49 \leqslant \nu \leqslant \nu_c$, the dependence of the coefficients μ_c, μ_2, and I_0 on the microscopic contact parameters can be deduced from the kinetic theory.

The yield stress ratio expression is given by Eq. (18). The value of μ_2 can be interpreted as the peak stress ratio shown in Figs. 7(d) and 8(d), which is the stress ratio at $\nu = 0.49$. Then, the dense limit of the ratio of Eq. (16) over Eq. (15), evaluated at $\nu = 0.49$, provides

$$\mu_2 = \left[\frac{24J_\infty\left(1-e_{\text{eff}}^2\right)}{5\pi(1+e_n)^2}\right]^{1/2}. \tag{19}$$

Finally, the coefficient I_0 is the value of the inertial number at which the stress ratio equals the intermediate value between μ_c and μ_2. This corresponds to a value, ν^*, of the solid volume fraction intermediate between ν_c and 0.49, which, from the dense limit of the ratio between Eqs. (16) and (15), is

$$\nu^* = \frac{26\pi(1+e_n)^2(1-e_{\text{eff}})(\mu_c+\mu_2)^2 0.49 - 15\pi(1+e_n)^2(\mu_c+\mu_2)^2 0.64 + 288J_\infty\left(1-e_{\text{eff}}^2\right)0.64}{26\pi(1+e_n)^2(1-e_{\text{eff}})(\mu_c+\mu_2)^2 - 15\pi(1+e_n)^2(\mu_c+\mu_2)^2 + 288J_\infty\left(1-e_{\text{eff}}^2\right)}. \tag{20}$$

Then, from Eqs. (15) and (16),

$$I_0 = \frac{5\pi^{1/2}(1+e_n)^{1/2}(\mu_c+\mu_2)}{2^{3/2}J_\infty\nu^*\chi_0^{*1/2}}, \tag{21}$$

where χ_0^* is the radial distribution function at contact evaluated at $\nu = \nu^*$.

IV. HETEROGENEOUS FLOWS: NONLOCAL RHEOLOGY AND KINETIC THEORY

As mentioned, the Bagnold or inertial rheology cannot apply in the absence of shearing, as in homogeneous cooling where random, inelastic collisions gradually dissipate the kinetic energy of the systems so that the granular temperature decays with time [9]. However, this rheology also fails under steady conditions, in the presence of heterogeneities.

Perhaps the simplest systems to observe these shortcomings are steady, gravity-driven flows over rigid beds in the absence of lateral confinement [Fig. 3(c)] and Couette flows, i.e., steady flows between parallel, rigid beds in relative motion in the absence of gravity [Fig. 3(d)]. In both cases, the momentum balance implies that the ratio of the shear stress to the pressure, μ^*, is uniformly distributed along the direction perpendicular to the flow, while DEM simulations [36,37,100,101] indicate that the solid volume fraction is a function of y: there is a dense core region where the solid volume fraction is large and approximately constant, surrounded by two more dilute (boundary) layers with significant variation in ν [Figs. 3(c) and 3(d)]. Obviously, neither Eqs. (10) and (11) nor Eqs. (12) and (13) can reproduce this behavior, given the lack of monotonicity of μ^* with ν. The thickness of these boundary layers is a few particle diameters [101]. Hence, in fairness, the inertial rheology can still do a good job in predicting the features of such flows, if they are thick enough, say, larger than 10–15 diameters, so that the core region dominates [102].

Figure 9 shows the pressure measured in DEM simulations of steady, inclined flows over erodible beds [74] and Couette flows between rigid, bumpy plates [36] as a function of the solid volume fraction, using either the Bagnold (equivalent to the inertial rheology) or the kinetic theory scaling. The data do not collapse onto a master curve if the Bagnold scaling is adopted [Figs. 9(a) and 9(c)], while they do with the kinetic theory scaling: the pressure is very well predicted by Eq. (2) over the entire range of solid volume fraction [Figs. 9(b) and 9(d)]. The scattering of the measurements when the Bagnold scaling is adopted is due to the fact that the one-to-one relation between the shear rate and the square root of the granular temperature [Eq. (14)] does not hold everywhere.

The shortcomings of the inertial rheology are even more evident in situations in which the granular material flows, i.e., the inertial number is nonzero, but the stress ratio is less than the yield, μ_c, as in vertical chutes [97], annular shear cells [11], and split-bottom cells [60].

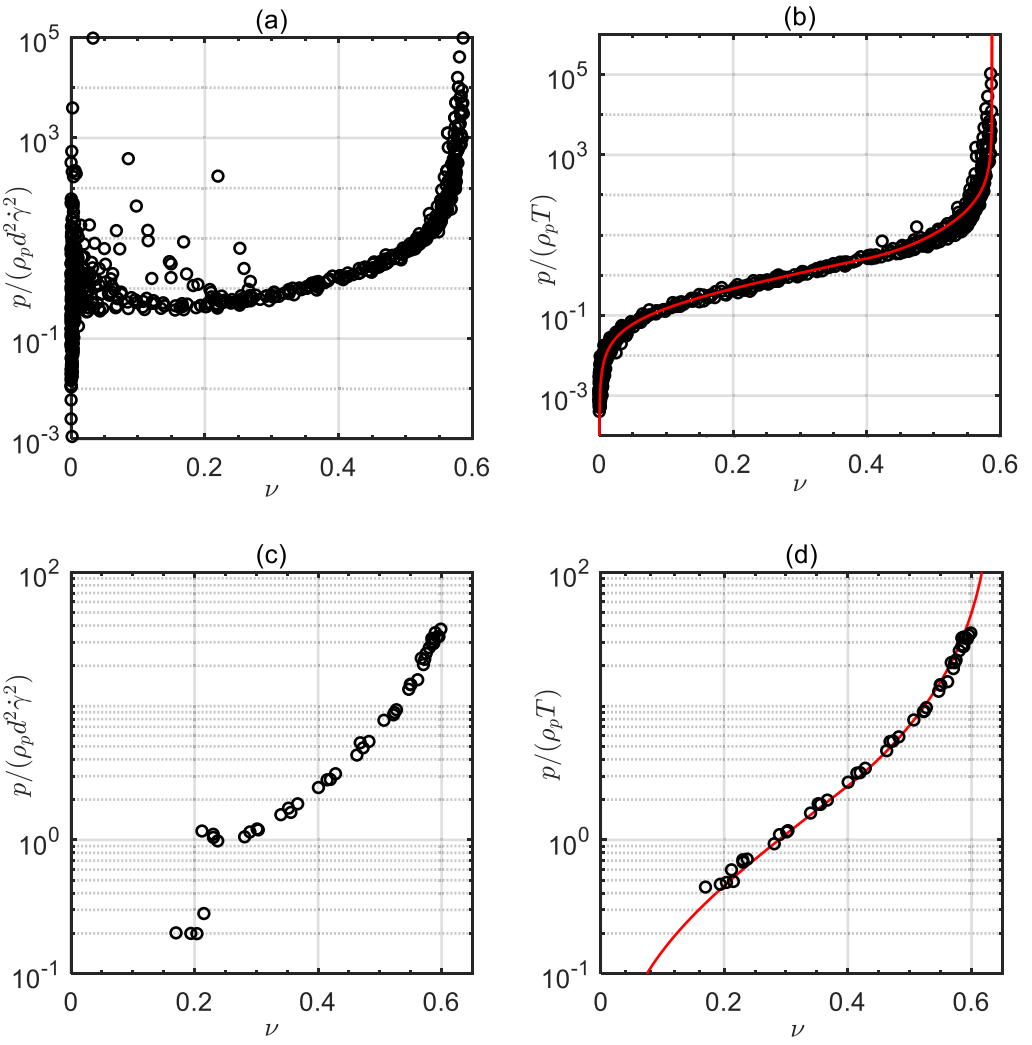

FIG. 9. Measurements (DEM simulations, black circles) [36,74] and predictions from kinetic theory [Eq. (2), red lines] of pressure in [(a) and (b)] steady, heterogeneous, gravity-driven flows over erodible beds with lateral confinement where $e_n = 0.88$, $e_t = 1$, $\mu = 0.5$, and $k_n \approx 3\times10^6\rho_p g d^2$ (angles of inclination between 24° and 55° and channel width between 10 and 30 particle diameters) and [(c) and (d)] Couette flows with $e_n = 0.8$, $e_t = 1$, $\mu = 0$, and $k_n = 2\times10^5\rho_p d V^2$. The data are plotted using [(a) and (c)] the Bagnold scaling and [(b) and (d)] the kinetic theory scaling.

By recognizing that the heterogeneities were the reason for the failure of the inertial rheology, various research groups have proposed to account for the so-called nonlocal effects in dense granular flows by either (i) a gradient expansion of the relation between μ^* and I [57],

$$\mu^* = \left(\mu_c + \frac{\mu_2 - \mu_c}{I_0 + I} I\right)\left(1 - \frac{b}{I} d^2 \nabla^2 I\right), \tag{22}$$

where b is an additional material-dependent parameter to be determined; or (ii) introducing a new hydrodynamic field, the granular fluidity $g = \dot{\gamma}/\mu^*$, and a balance for it, that, at least under steady

conditions [59,60], is

$$\xi^2 \nabla^2 g = g - g_{loc}, \tag{23}$$

where

$$g_{loc} = \frac{I_0}{\mu^*} \frac{\mathrm{H}(\mu^* - \mu_c)(\mu^* - \mu_c)}{\mu_2 - \mu^*} \sqrt{\frac{p}{\rho_p d^2}} \tag{24}$$

is the local value of the fluidity, which permits to recover the inertial rheology, Eq. (11), under homogeneous conditions. The Heaviside function is introduced because g_{loc} is taken to vanish if the stress ratio is less than the yield value, as in flows with $\nu > \nu_c$. The material parameter ξ is a cooperativity length for plastic rearrangement [60], and is taken to be proportional to the particle diameter d through a function of μ^* that is singular at μ_c [60]. An extension of this nonlocal granular fluidity (NGF) model to deal with unsteadiness has also been proposed [56].

Both Eqs. (22) and (23) are similar in spirit: they deal with dense, heterogeneous flows by introducing Laplacian terms, i.e., diffusive terms, either in the inertial number or in the granular fluidity, and, therefore, turning an algebraic into a second-order differential equation. In so doing, they lose the advantage of the inertial rheology with respect to the kinetic theory, because the number of differential equations that are to be solved is identical. More importantly, boundary conditions on I and its derivative, or g and its derivative, must be provided. Due to the definitions of the inertial number and the granular fluidity, these boundary conditions are conditions on the first derivative and the second derivative of the particle velocity at the boundary, whose physical meaning is unclear. Indeed, successful applications of the NGF model have been obtained by taking the simple conditions $g = g_{loc}$ and $\partial_y g = 0$ at the boundaries [56,59,60], without accounting for, e.g., the actual geometrical features of the boundary itself. Moreover, once the granular fluidity field is determined, usually in situations for which the stress fields are simple enough to be used as inputs, the particle velocity field can be determined only if the value of the velocity is known at the boundary. Once again, this is either simply taken to be zero, which works for extremely rough surfaces, or is taken from the DEM simulations and not predicted [57,59].

Boundary conditions for the kinetic theory, that allow also the determination of the slip velocity, can be derived, instead, from the usual balances of fluctuation kinetic energy and momentum phrased at the boundaries, taking into account their geometry and microscopic properties [69,103,104]. The dense limit of the balance of fluctuation kinetic energy, Eq. (5), under steady conditions, is

$$\frac{\dot\gamma p}{\Gamma s} \nabla \cdot \left(\rho_p \frac{4 M_\infty \nu^2 \chi_0}{\pi^{1/2}} d 2T \nabla T^{1/2} \right) = \frac{\dot\gamma p}{s} - \frac{\dot\gamma p}{\Gamma/\dot\gamma}, \tag{25}$$

with Eq. (6), neglecting the term proportional to the gradient of ν in dense conditions, and

$$M = M_\infty \approx \frac{1+e_n}{2} + \frac{9\pi}{8} \frac{(1+e_n)^3(2e_n - 1)}{16(1+e_n) - 7\left(1-e_n^2\right)}. \tag{26}$$

By defining, with Eqs. (2), (3), and (8) in the dense limit,

$$g = \frac{\dot\gamma p}{s} \approx \frac{5\pi^{1/2}}{2} \frac{T^{1/2}}{d} \tag{27}$$

and

$$g_{loc} = \frac{\dot\gamma p}{\Gamma/\dot\gamma} \approx \frac{\pi^{1/2}(1+e_n)}{6\left(1-e_{\mathrm{eff}}^2\right)} \frac{L}{d} \frac{\dot\gamma^2 d}{T^{1/2}}, \tag{28}$$

Eq. (25) can be rewritten as

$$\frac{1}{3\rho_p\left(1-e_{\mathrm{eff}}^2\right)\nu^2\chi_0 T} \frac{M_\infty}{1+e_n} \frac{L}{d} d^2 \nabla \cdot (p \nabla g) = g - g_{loc}. \tag{29}$$

The local value of the granular fluidity, Eq. (28), is defined by substituting, in the expression of g, the shear stress, s, with the ratio of the dissipation rate over the shear rate, $\Gamma/\dot{\gamma}$. Then, the condition $g = g_{loc}$ coincides with the algebraic balance between the energy production and the energy dissipation that results in Eq. (14). From there, both the Bagnold rheology, Eqs. (12) and (13), and the inertial rheology, from the constitutive relations of the kinetic theory [Eqs. (2) and (3)], are recovered.

If ∇p is small, Eq. (29) takes the final form

$$\frac{2M_\infty}{3\left(1-e_{\text{eff}}^2\right)}\frac{L}{d}d^2\nabla^2 g = g - g_{loc}, \tag{30}$$

that is exactly Eq. (23) with an explicit expression for the cooperativity length,

$$\xi = \sqrt{\frac{2M_\infty}{3\left(1-e_{\text{eff}}^2\right)}\frac{L}{d}}d. \tag{31}$$

Using the energy balance of kinetic theory, it is natural to identify the diffusive term involving the granular fluidity in the NGF model as the diffusion of fluctuation kinetic energy induced by the velocity fluctuations.

The algebraic relation between the granular fluidity and the square root of the granular temperature, Eq. (27), has been already proved in DEM simulations [66]. The ratio $g/T^{1/2}$ was actually shown to depend on the solid volume fraction as the critical value is approached, and this behavior can be captured if one employs kinetic theories that provide constitutive relations for the stresses that include terms that are quadratic in the shear rate [105]. Here, the analysis is limited to kinetic theories that are linear in the shear rate, and Eq. (27) is a sufficiently good approximation.

Interestingly, Eq. (30) was obtained by employing the constitutive relations for the stresses, the fluctuation energy flux, and the collisional dissipation rate valid for dense, subcritical ($\nu < \nu_c$) flows of hard spheres. However, the exact same equation holds even if the finite contact duration associated with the finite particle stiffness [39] is included, because p, s, $\mathbf{Q}$, and Γ would all be proportional to the stiffness-dependent frequency of collisions. Perhaps more importantly, Eq. (30) is also valid for supercritical ($\nu > \nu_c$) flows, with the reasonable assumption that the fluctuation kinetic energy is produced through the work of only the rate-dependent component of the shear stress, and that s and p in Eqs. (27) and (28) are, then, to be understood as the rate-dependent components of the stresses [39]. DEM simulations [39,76] of steady, homogeneous, supercritical flows suggest that the correlation length, L, is approximately constant there and equal to

$$\left.\frac{L}{d}\right|_{\nu\geqslant\nu_c} = 1 + \frac{26(1-e_{\text{eff}})}{15}\frac{\nu_c - 0.49}{0.64-\nu_c}. \tag{32}$$

The magnitude of the cooperativity length $\xi = \sqrt{(g-g_{loc})/\nabla^2 g}$, from Eq. (23), can be inferred from local measurements of T and $\dot{\gamma}$ at $\nu \geqslant \nu_c$ in DEM simulations of steady, heterogeneous flows, using Eqs. (27), (28), and (32). In so doing, one must pay particular attention in that the evaluation of the Laplacian term, $\nabla^2 g$, requires the determination of the second spatial derivative of $T^{1/2}$, given the definition of g in Eq. (27), and that greatly magnifies any numerical errors already present in the data.

Figure 10 shows the supercritical cooperativity length as a function of the solid volume fraction and the stress ratio extracted from DEM simulations [74] of inclined flows over erodible beds [Fig. 3(c)] over a large range of angles of inclinations. The measurements of granular temperature and velocity, needed to evaluate g and g_{loc}, have been smoothed using a Gaussian-weighted moving average over a window equal to eight data points. Despite the residual scattering, the cooperativity length is in good agreement with Eq. (31).

It is worth emphasizing that, in the framework of the kinetic theory, it is not necessary to assume that g_{loc} vanishes when the stress ratio is less than the yield: Eq. (28) retains its validity, regardless of the value of μ^*. Also, as suggested by Eq. (31) with Eq. (32), the cooperativity length at $\nu \geqslant \nu_c$ is

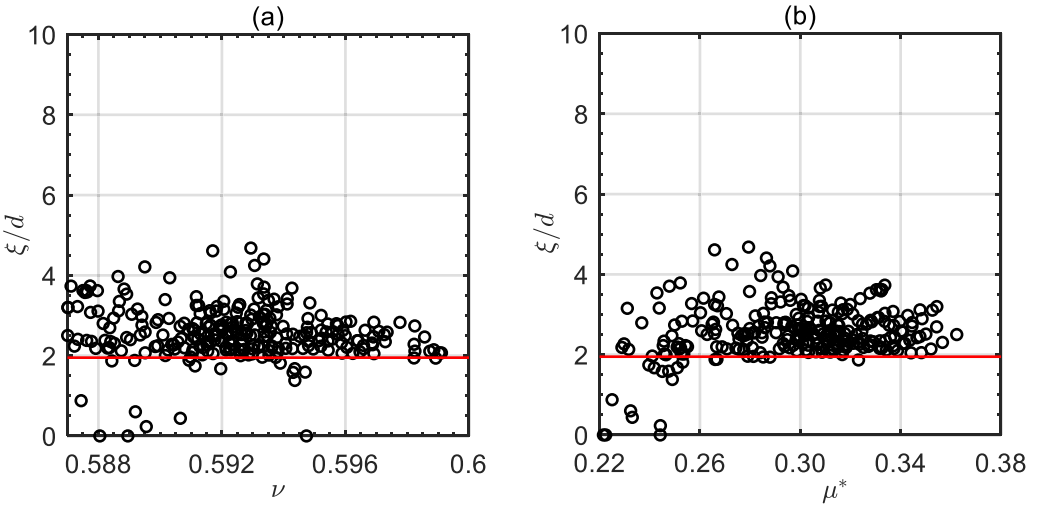

FIG. 10. Cooperativity length as a function of (a) the solid volume fraction and (b) the stress ratio inferred from DEM simulations (black circles) [74] of steady, heterogeneous, gravity-driven flows over erodible beds with lateral confinement at $\nu \geqslant \nu_c$ ($e_n = 0.88$, $e_t = 1$, $\mu = 0.5$, $k_n \approx 3\times10^6 \rho_p g d^2$, angles of inclination between 24° and 55°, and channel width between 10 and 30 particle diameters) and predicted from the kinetic theory [Eq. (31), red lines].

approximately constant and shows no sign of singular behavior at $\mu^* = \mu_c \approx 0.38$ (from Eq. (18), with $\nu_c = 0.587$ when $\mu = 0.5$ [80]).

V. CONCLUSIONS

As bluntly pointed out in a review paper on dense granular flows back in 2008, whereas "classical fluids are well described by the Navier-Stokes equations, no constitutive law can reproduce the diversity of behavior observed with a cohesionless granular material" [43]. This opinion is still widely spread among the research community, and it is hard to find a paper without a generic sentence in its introduction about the lack of universally valid constitutive relations of stresses in granular flows.

A synthesis of previously published results under steady conditions has permitted to conclude that the kinetic theory of granular gases, extended to account for the breaking of the molecular chaos assumption through a correlation length and the role of particle friction through an effective coefficient of restitution, offers indeed a universal framework to describe the flows of realistic grains from dilute up to very dense conditions. The upper limit is set by the critical volume fraction, above which rate-independent components of the stresses, proportional to the particle stiffness, appear. Given that realistic particles are rather stiff, DEM simulations have revealed that, in the subcritical regime, the stresses originate from momentum exchange in collisions, and the collisions are binary and almost instantaneous, contrary to popular belief. In the supercritical regime, on the other hand, the rate-independent components of the stresses dominate. The transition from the subcritical to the supercritical regime is so abrupt for particles of realistic stiffness that it seems convenient to model flows in which the two regimes coexist through two spatially distinct domains.

Perhaps more rigorously than in previous works, it has been shown how the inertial rheology and Bagnold's rheology are special cases of the kinetic theory of granular gases applied to steady, homogeneous flows. This has allowed the determination of the dependence of the material parameters in the inertial rheology on the microscopic contact properties of the particles, i.e., the coefficients of collisional restitution and friction.

The nonlocal granular fluidity model, proposed to extend the inertial rheology to heterogeneous flows, has also been derived from the kinetic theory of granular gases. The differential equation for the granular fluidity coincides with the balance of fluctuation energy of the kinetic theory, with the granular fluidity proportional to the square root of the granular temperature, and has been shown to be valid in both the subcritical and supercritical regimes. In the latter, indeed, although the rate-independent components of the stresses dominate, the velocity fluctuations are still crucial in determining the diffusions of momentum and energy that, in turn, permit the particles to flow. When applied to DEM simulations of steady, heterogeneous, flows driven by gravity, the NGF model derived from the kinetic theory has the advantages that the local fluidity must not be assumed to vanish in the supercritical regime, and that the cooperativity length is constant there and does not diverge when the stress ratio approaches its yield value, at the onset of the rate-independent components of the stresses. Indeed, the link between the cooperativity length of the NGF model and the correlation length of the kinetic theory has been made explicit.

There are still issues that need to be clarified and addressed. The kinetic theory of granular gases relies on two physical quantities, the radial distribution function at contact and the correlation length, for which, at the moment, only phenomenological expressions are available. The only parameters in these expressions are the microscopic contact properties of the particles; nonetheless, it would be desirable to directly measure the radial distribution function at contact and the correlation length in numerical simulations, as done in a few cases in the past, and systematically investigate their dependence on the coefficients of restitution and friction. Also, the dependence of key values of the solid volume fraction, such as the random close packing, and the critical and the freezing points, on polydispersity and shape remains to be determined.

So far, extensive tests of the kinetic theory of granular gases have been mostly carried out on steady flows with divergence-free velocity fields: shifting the focus to unsteadiness and expanding or contracting flows, where the volumetric viscosity must play an important role, is the next natural step.

Finally, the realm of the kinetic theory, with its hydrodynamic fields—solid volume fraction, velocity, and granular temperature—must be further extended to incorporate additional fields, such as the coordination number and the fabric tensor, in the hope to describe unsteady and/or heterogeneous situations in which, e.g., velocity fluctuations progressively diffuse into the skeleton of a solidlike granular assembly and cause it to flow (onset or erosion processes), or a network of long-lasting contacts develops in the granular material and resists the flow (arrest or deposition).

[1] I. Goldhirsch, Rapid granular flows, Annu. Rev. Fluid Mech. **35**, 267 (2003).
[2] A. J. Liu and S. R. Nagel, Jamming is not just cool any more, Nature (London) **396**, 21 (1998).
[3] R. Bagnold, *The Physics of Blown Sand and Desert Dunes* (Methuen, New York, 1941).
[4] R. Bagnold, Experiments on a gravity-free dispersion of large solid spheres in a Newtonian fluid under shear, Proc. R. Soc. London Ser. A **225**, 49 (1954).
[5] R. Bagnold, An approach to the sediment transport problem from general physics, US government printing office (1966).
[6] J. T. Jenkins and D. Berzi, Kinetic theory applied to inclined flows, Granular Matter **14**, 79 (2012).
[7] C. S. Campbell, Rapid granular flows, Annu. Rev. Fluid Mech. **22**, 57 (1990).
[8] D. McTigue, Mixture theory for suspended sediment transport, J. Hydr. Div. **107**, 659 (1981).
[9] I. Goldhirsch, Introduction to granular temperature, Powder Technol. **182**, 130 (2008).
[10] D. Bi, J. Zhang, B. Chakraborty, and R. P. Behringer, Jamming by shear, Nature (London) **480**, 355 (2011).
[11] G. Koval, J.-N. Roux, A. Corfdir, and F. Chevoir, Annular shear of cohesionless granular materials: From the inertial to quasistatic regime, Phys. Rev. E **79**, 021306 (2009).

[12] J. N. Roux and G. Combe, Quasistatic rheology and the origins of strain, C. R. Phys. **3**, 131 (2002).
[13] D. Wood, *Soil Mechanics: A One-Dimensional Introduction* (Cambridge University Press, Cambridge, UK, 2009).
[14] S. Savage and D. J. Jeffrey, The stress tensor in a granular flow, J. Fluid Mech. **110**, 255 (1981).
[15] P. K. Haff, Grain flow as a fluid-mechanical phenomenon, J. Fluid Mech. **134**, 401 (1983).
[16] J. Jenkins and S. Savage, A theory for the rapid flow of identical, smooth, nearly elastic, spherical particles, J. Fluid Mech. **130**, 187 (1983).
[17] S. Savage and M. Sayed, Stresses developed by dry cohesionless granular materials sheared in an annular shear cell, J. Fluid Mech. **142**, 391 (1984).
[18] C. K. K. Lun, S. B. Savage, D. J. Jeffrey, and N. Chepurniy, Kinetic theories for granular flow: Inelastic particles in Couette flow and slightly inelastic particles in a general flowfield, J. Fluid Mech. **140**, 223 (1984).
[19] J. T. Jenkins and M. W. Richman, Kinetic theory for plane flows of a dense gas of identical, rough, inelastic, circular disks, Phys. Fluids **28**, 3485 (1985).
[20] C. Lun, Kinetic theory for granular flow of dense, slightly inelastic, slightly rough spheres, J. Fluid Mech. **233**, 539 (1991).
[21] J. T. Jenkins and C. Zhang, Kinetic theory for identical, frictional, nearly elastic spheres, Phys. Fluids **14**, 1228 (2002).
[22] M. Larcher and J. T. Jenkins, Segregation and mixture profiles in dense, inclined flows of two types of spheres, Phys. Fluids **25**, 113301 (2013).
[23] V. Garzó and J. W. Dufty, Dense fluid transport for inelastic hard spheres, Phys. Rev. E **59**, 5895 (1999).
[24] J. T. Jenkins and M. W. Richman, Plane simple shear of smooth inelastic circular disks: The anisotropy of the second moment in the dilute and dense limits, J. Fluid Mech. **192**, 313 (1988).
[25] M. Alam and S. Luding, First normal stress difference and crystallization in a dense sheared granular fluid, Phys. Fluids **15**, 2298 (2003).
[26] M. Alam and S. Luding, in *Powders and Grains*, edited by R. Garcia-Rojo, H. J. Herrmann, and S. McNamara (A. A. Balkema, London, 2005), pp. 1141–1144.
[27] S. Saha and M. Alam, Normal stress differences, their origin and constitutive relations for a sheared granular fluid, J. Fluid Mech. **795**, 549 (2016).
[28] S. Saha and M. Alam, Burnett-order constitutive relations, second moment anisotropy and co-existing states in sheared dense gas-solid suspensions, J. Fluid Mech. **887**, A9 (2020).
[29] N. Mitarai and H. Nakanishi, Bagnold scaling, density plateau, and kinetic theory analysis of dense granular flow, Phys. Rev. Lett. **94**, 128001 (2005).
[30] N. Mitarai and H. Nakanishi, Velocity correlations in dense granular shear flows: Effects on energy dissipation and normal stress, Phys. Rev. E **75**, 031305 (2007).
[31] S. Torquato, Nearest-neighbor statistics for packings of hard spheres and disks, Phys. Rev. E **51**, 3170 (1995).
[32] J. T. Jenkins, Dense shearing flows of inelastic disks, Phys. Fluids **18**, 103307 (2006).
[33] J. T. Jenkins, Dense inclined flows of inelastic spheres, Granular Matter **10**, 47 (2007).
[34] J. T. Jenkins and D. Berzi, Dense inclined flows of inelastic spheres: Tests of an extension of kinetic theory, Granular Matter **12**, 151 (2010).
[35] D. Berzi and J. T. Jenkins, Surface flows of inelastic spheres, Phys. Fluids **23**, 013303 (2011).
[36] D. Vescovi, D. Berzi, P. Richard, and N. Brodu, Plane shear flows of frictionless spheres: Kinetic theory and 3D soft-sphere discrete element method simulations, Phys. Fluids **26**, 053305 (2014).
[37] D. Gollin, D. Berzi, and E. T. Bowman, Extended kinetic theory applied to inclined granular flows: Role of boundaries, Granular Matter **19**, 56 (2017).
[38] H. Hwang and K. Hutter, A new kinetic model for rapid granular flow, Continuum Mech. Thermodyn. **7**, 357 (1995).
[39] D. Berzi and J. T. Jenkins, Steady shearing flows of deformable, inelastic spheres, Soft Matter **11**, 4799 (2015).
[40] D. Berzi, N. Thai-Quang, Y. Guo, and J. Curtis, Stresses and orientational order in shearing flows of granular liquid crystals, Phys. Rev. E **93**, 040901(R) (2016).

[41] D. Berzi, N. Thai-Quang, Y. Guo, and J. Curtis, Collisional dissipation rate in shearing flows of granular liquid crystals, Phys. Rev. E **95**, 050901(R) (2017).
[42] O. Pouliquen and F. Chevoir, Dense flows of dry granular material, C. R. Phys. **3**, 163 (2002).
[43] Y. Forterre and O. Pouliquen, Flows of dense granular media, Annu. Rev. Fluid Mech. **40**, 1 (2008).
[44] G. D. R. Midi, On dense granular flows, Eur. Phys. J. E **14**, 341 (2004).
[45] P. Jop, Y. Forterre, and O. Pouliquen, Crucial role of side walls for granular surface flows: Consequences for the rheology, J. Fluid Mech. **541**, 167 (2005).
[46] F. da Cruz, S. Emam, M. Prochnow, J.-N. Roux, and F. Chevoir, Rheophysics of dense granular materials: Discrete simulation of plane shear flows, Phys. Rev. E **72**, 021309 (2005).
[47] P. Y. Lagrée, L. Staron, and S. Popinet, The granular column collapse as a continuum: Validity of a two-dimensional Navier-Stokes model with a $\mu(I)$-rheology, J. Fluid Mech. **686**, 378 (2011).
[48] E. Rojas, M. Trulsson, B. Andreotti, E. Clément, and R. Soto, Relaxation processes after instantaneous shear-rate reversal in a dense granular flow, Europhys. Lett. **109**, 64002 (2015).
[49] M. Ouriemi, P. Aussillous, and É. Guazzelli, Sediment dynamics. Part 1. Bed-load transport by laminar shearing flows, J. Fluid Mech. **636**, 295 (2009).
[50] F. Chiodi, P. Claudin, and B. Andreotti, A two phase flow model of sediment transport: Transition from bed-load to suspended-load, J. Fluid Mech. **755**, 561 (2014).
[51] T. Barker, M. Rauter, E. S. Maguire, C. G. Johnson, and J. M. Gray, Coupling rheology and segregation in granular flows, J. Fluid Mech. **909**, A22 (2021).
[52] F. Boyer, É. Guazzelli, and O. Pouliquen, Unifying suspension and granular rheology, Phys. Rev. Lett. **107**, 188301 (2011).
[53] M. Trulsson, B. Andreotti, and P. Claudin, Transition from the viscous to inertial regime in dense suspensions, Phys. Rev. Lett. **109**, 118305 (2012).
[54] D. B. Nagy, P. Claudin, T. Börzsönyi, and E. Somfai, Rheology of dense granular flows for elongated particles, Phys. Rev. E **96**, 062903 (2017).
[55] A. J. Holyoake and J. N. McElwaine, High-speed granular chute flows, J. Fluid Mech. **710**, 35 (2012).
[56] K. Kamrin and D. L. Henann, Nonlocal modeling of granular flows down inclines, Soft Matter **11**, 179 (2015).
[57] M. Bouzid, M. Trulsson, P. Claudin, E. Clément, and B. Andreotti, Nonlocal rheology of granular flows across yield conditions, Phys. Rev. Lett. **111**, 238301 (2013).
[58] M. Bouzid, A. Izzet, M. Trulsson, E. Clément, P. Claudin, and B. Andreotti, Non-local rheology in dense granular flows, Eur. Phys. J. E **38**, 125 (2015).
[59] K. Kamrin and G. Koval, Nonlocal Constitutive Relation for Steady Granular Flow, Phys. Rev. Lett. **108**, 178301 (2012).
[60] D. Henann and K. Kamrin, A predictive, size-dependent continuum model for dense granular flows, Proc. Natl. Acad. Sci. USA **110**, 6730 (2013).
[61] P. Jop, Y. Forterre, and O. Pouliquen, A constitutive law for dense granular flows, Nature (London) **441**, 727 (2006).
[62] S. Kim and K. Kamrin, A second-order non-local model for granular flows, Front. Phys. **11**, 1 (2023).
[63] V. Ogarko and S. Luding, Prediction of polydisperse hard-sphere mixture behavior using tridisperse systems, Soft Matter **9**, 9530 (2013).
[64] R. C. Hidalgo, B. Szabó, K. Gillemot, T. Börzsönyi, and T. Weinhart, Rheological response of nonspherical granular flows down an incline, Phys. Rev. Fluids **3**, 074301 (2018).
[65] D. Berzi and D. Vescovi, Different singularities in the functions of extended kinetic theory at the origin of the yield stress in granular flows, Phys. Fluids **27**, 013302 (2015).
[66] Q. Zhang and K. Kamrin, Microscopic description of the granular fluidity field in nonlocal flow modeling, Phys. Rev. Lett. **118**, 058001 (2017).
[67] J. T. Jenkins, M. Alam, and D. Berzi, Singular behavior of the stresses in the limit of random close packing in collisional, simple shearing flows of frictionless spheres, Phys. Rev. Fluids **5**, 072301(R) (2020).
[68] O. R. Walton, Numerical simulation of inelastic, frictional particle- particle interactions, in *Particulate Two-Phase Flow*, edited by M. C. Roco (Butterworth-Heinemann, London, 1992), pp. 1249–1253.

[69] J. T. Jenkins, Boundary conditions for rapid granular flow: Flat, frictional walls, J. Appl. Mech. **59**, 120 (1992).
[70] S. F. Foerster, M. Y. Louge, H. Chang, and K. Allia, Measurements of the collision properties of small spheres, Phys. Fluids **6**, 1108 (1994).
[71] P. A. Cundall and O. D. L. Strack, A discrete numerical model for granular assemblies, Géotechnique **29**, 47 (1979).
[72] S. Chapman and T. Cowling, The Mathematical Theory of Non-Uniform Gases: An Account of the Kinetic Theory of Viscosity, Thermal Conduction and Diffusion in Gases (Cambridge University Press, Cambridge, UK, 1990).
[73] N. Carnahan and K. Starling, Equation of state for nonattracting rigid spheres, J. Chem. Phys. **51**, 635 (1969).
[74] D. Berzi, J. T. Jenkins, and P. Richard, Extended kinetic theory for granular flow over and within an inclined erodible bed, J. Fluid Mech. **885**, A27 (2020).
[75] O. Herbst, M. Huthmann, and A. Zippelius, Dynamics of inelastically colliding spheres with Coulomb friction: Relaxation of translational and rotational energy, Granular Matter **2**, 211 (2000).
[76] N. Oyama, H. Mizuno, and K. Saitoh, Avalanche interpretation of the power-law energy spectrum in three-dimensional dense granular flow, Phys. Rev. Lett. **122**, 188004 (2019).
[77] D. Berzi, Extended kinetic theory applied to dense, granular, simple shear flows, Acta Mech. **225**, 2191 (2014).
[78] M. Babic, H. H. Shen, and H. T. Shen, The stress tensor in granular shear flows of uniform, deformable disks at high solids concentrations, J. Fluid Mech. **219**, 81 (1990).
[79] S. Ji and H. H. Shen, Internal parameters and regime map for soft polydispersed granular materials, J. Rheol. **52**, 87 (2008).
[80] S. Chialvo, J. Sun, and S. Sundaresan, Bridging the rheology of granular flows in three regimes, Phys. Rev. E **85**, 021305 (2012).
[81] P. Johnson, P. Nott, and R. Jackson, Frictional-collisional equations of motion for particulate flows and their application to chutes, J. Fluid Mech. **210**, 501 (1990).
[82] D. Berzi, J. T. Jenkins, and P. Richard, Erodible, granular beds are fragile, Soft Matter **15**, 7173 (2019).
[83] C. Song, P. Wang, and H. A. Makse, A phase diagram for jammed matter: Supplementary information, Nature (London) **453**, 629 (2008).
[84] L. E. Silbert, Jamming of frictional spheres and random loose packing, Soft Matter **6**, 2918 (2010).
[85] J. Sun and S. Sundaresan, A constitutive model with microstructure evolution for flow of rate-independent granular materials, J. Fluid Mech. **682**, 590 (2011).
[86] D. Vescovi and S. Luding, Merging fluid and solid granular behavior, Soft Matter **12**, 8616 (2016).
[87] D. Berzi, K. E. Buettner, and J. S. Curtis, Dense shearing flows of soft, frictional cylinders, Soft Matter **18**, 80 (2022).
[88] D. Vescovi, D. Berzi, and C. di Prisco, Fluid-solid transition in unsteady, homogeneous, granular shear flows, Granular Matter **20**, 27 (2018).
[89] D. Howell, R. P. Behringer, and C. Veje, Stress fluctuations in a 2D granular Couette experiment: A continuous transition, Phys. Rev. Lett. **82**, 5241 (1999).
[90] S. Schöllmann, Simulation of a two-dimensional shear cell, Phys. Rev. E **59**, 889 (1999).
[91] S. Ji, D. M. Hanes, and H. H. Shen, Comparisons of physical experiment and discrete element simulations of sheared granular materials in an annular shear cell, Mech. Mater. **41**, 764 (2009).
[92] A. Armanini, H. Capart, L. Fraccarollo, and M. Larcher, Rheological stratification in experimental free-surface flows of granular-liquid mixtures, J. Fluid Mech. **532**, 269 (2005).
[93] O. Pouliquen and Y. Forterre, A non-local rheology for dense granular flows, Philos. Trans. Ser. A **367**, 5091 (2009).
[94] S. Schneiderbauer, A. Aigner, and S. Pirker, A comprehensive frictional-kinetic model for gas-particle flows: Analysis of fluidized and moving bed regimes, Chem. Eng. Sci. **80**, 279 (2012).
[95] P. Jop, Rheological properties of dense granular flows, C. R. Phys. **16**, 62 (2015).
[96] R. Chassagne, C. Bonamy, and J. Chauchat, A frictional-collisional model for bedload transport based on kinetic theory of granular flows: Discrete and continuum approaches, J. Fluid Mech. **964**, A27 (2023).

[97] M. U. Islam, J. T. Jenkins, and S. L. Das, Extended kinetic theory for granular flow in a vertical chute, J. Fluid Mech. **950**, A13 (2022).
[98] S. Chialvo and S. Sundaresan, A modified kinetic theory for frictional granular flows in dense and dilute regimes, Phys. Fluids **25**, 070603 (2013).
[99] T. Barker, D. G. Schaeffer, P. Bohorquez, and J. M. Gray, Well-posed and ill-posed behaviour of the μ-rheology for granular flow, J. Fluid Mech. **779**, 794 (2015).
[100] L. E. Silbert, D. Ertas, G. S. Grest, T. C. Halsey, D. Levine, and S. J. Plimpton, Granular flow down an inclined plane: Bagnold scaling and rheology, Phys. Rev. E **64**, 051302 (2001).
[101] V. Kumaran, Dense granular flow down an inclined plane: From kinetic theory to granular dynamics, J. Fluid Mech. **599**, 121 (2008).
[102] O. Pouliquen, Scaling laws in granular flows down rough inclined planes, Phys. Fluids **11**, 542 (1999).
[103] M. W. Richman, Boundary conditions based upon a modified Maxwellian velocity distribution for flows of identical, smooth, nearly elastic spheres, Acta Mech. **75**, 227 (1988).
[104] J. T. Jenkins and E. Askari, Boundary conditions for rapid granular flows: Phase interfaces, J. Fluid Mech. **223**, 497 (1991).
[105] D. Berzi and J. T. Jenkins, Fluidity, anisotropy, and velocity correlations in frictionless, collisional grain flows, Phys. Rev. Fluids **3**, 094303 (2018).